NAA-SR-11762

COPY

DEVELOPMENT OF A SOLID STATE NEUTRON DETECTOR FOR SNAP 10A

AEC Research and Development Report

ATOMICS INTERNATIONAL
A DIVISION OF NORTH AMERICAN AVIATION, INC.

NAA-SR-11762
INSTRUMENTS TID-4500
41 PAGES

DEVELOPMENT OF A SOLID STATE NEUTRON DETECTOR FOR SNAP 10A

By
A. CHESAVAGE

ATOMICS INTERNATIONAL
A DIVISION OF NORTH AMERICAN AVIATION, INC.

CONTRACT: AT(11-1)-GEN-8
ISSUED: MAR 25 1966

DISTRIBUTION

This report has been distributed according to the category "Instruments" as given in the Standard Distribution for Unclassified Scientific and Technical Reports, TID-4500. The edition used was the one currently in effect on the date this document was issued.

CONTENTS

CONTENTS

TABLES

FIGURES

ABSTRACT

Electronic devices, primarily semiconductors, degrade in a nuclear radiation environment. In a reactor environment most of the damage is due to fast neutrons. The lithium hydride shield on SNAP 10A was designed to attenuate the fast neutron exposure at the instrument compartment to a tolerable level. To evaluate shield effectiveness fast neutron detectors were developed. Eight detectors were installed in the SNAP 10A FS-4 flight system. This report discusses the development and in-flight data of these detectors.

Each detector consisted of a 2N697 transistor as the variable leg in a bridge circuit. The complete detector was 1-1/4 x 1-1/4 x 3/4 in., consumed 0.26 watts, and weighed less than 3 oz with wiring. The degradation of transistor gain was correlated to integrated fast neutron flux in ground tests. These ground test data were used to reduce flight data.

During final qualification testing, it was found that the detectors were extremely gamma sensitive. For the comparatively low fast-neutron/gamma ratio in the SNAP 10A instrument compartment, the high gamma sensitivity decreased the detector's accuracy at mid-scale from about ±15% to accuracies ranging from ±35 to ±60%, depending on the fast neutron/gamma ratio.

The data from the 43-day flight of the SNAP 10A FS-4 system indicated fast neutron fluxes (>0.1 Mev) ranging from 0.64×10^6 n/cm^2-sec to 1.82×10^6 n/cm^2-sec in the instrument compartment. The exposures integrated for 43 days ranged from 2.4×10^{12} to 6.8×10^{12} nvt. The exposures extrapolated for one year range from 2.0×10^{13} to 5.7×10^{13} nvt.

I. FAST NEUTRON DETECTOR REQUIREMENTS

A. GENERAL

Electronic components, primarily semiconductors, degrade in the nuclear radiation environment of nuclear reactors and space. For the SNAP 10A-Agena vehicle (Figure 1) the space nuclear environment was insignificant compared with the nuclear reactor environment. All of the Atomics International electronic equipment on SNAP 10A was radiation hardened and ground qualification tested to larger exposures than the one-year extrapolated exposure herein reported.

B. CALCULATED FAST NEUTRON FLUXES IN THE SNAP 10A INSTRUMENT COMPARTMENT

The neutron shield was designed for a uniform flux rate in the instrument compartment due to direct shield penetration. Later calculations showed that scatter from the control drum projections and the converter were significant. The scatter components distorted the uniform flux rate pattern and resulted in relatively steep flux gradients across the instrument compartment. Figure 2[1] shows the reported fast neutron (>0.1 Mev) isodose map at the instrument compartment. More sophisticated calculations later indicated that the flux gradients were not as steep as shown in Figure 2. However, the need for measuring the flux pattern in the instrument compartment was evident. The application suggested a series of fast neutron detectors judiciously located to take full advantage of the symmetry present.

C. THERMAL VACUUM ENVIRONMENT

The detector had to withstand the usual shock and vibration environments encountered during launch. In orbit the detector would be operating in a space vacuum environment at about 110 to 130°F.

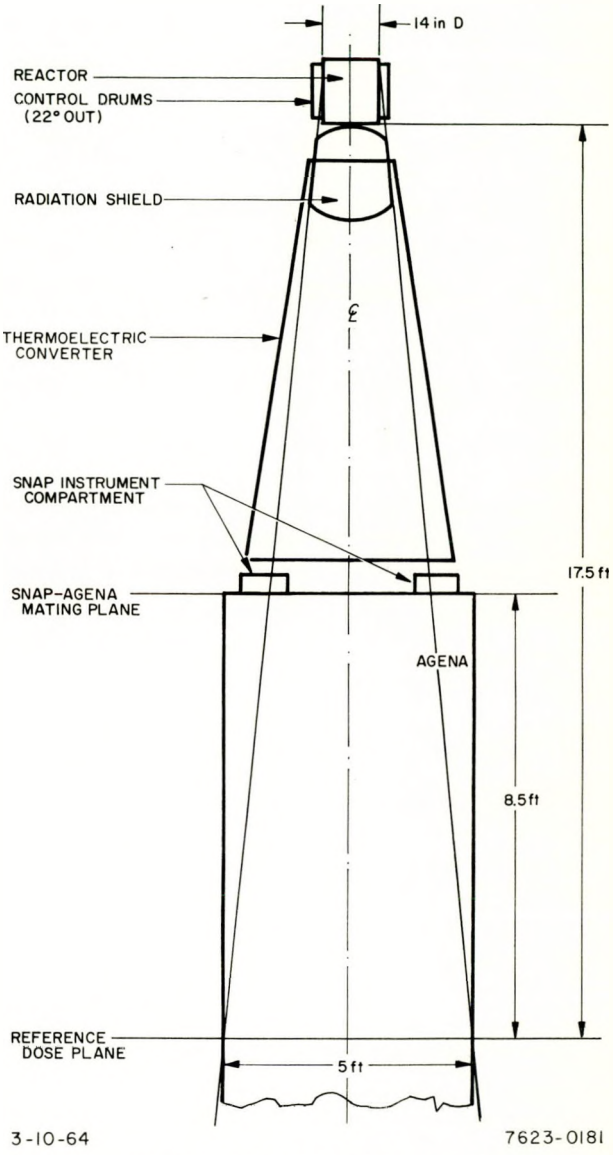

Figure 1. SNAP 10A-Agena Vehicle

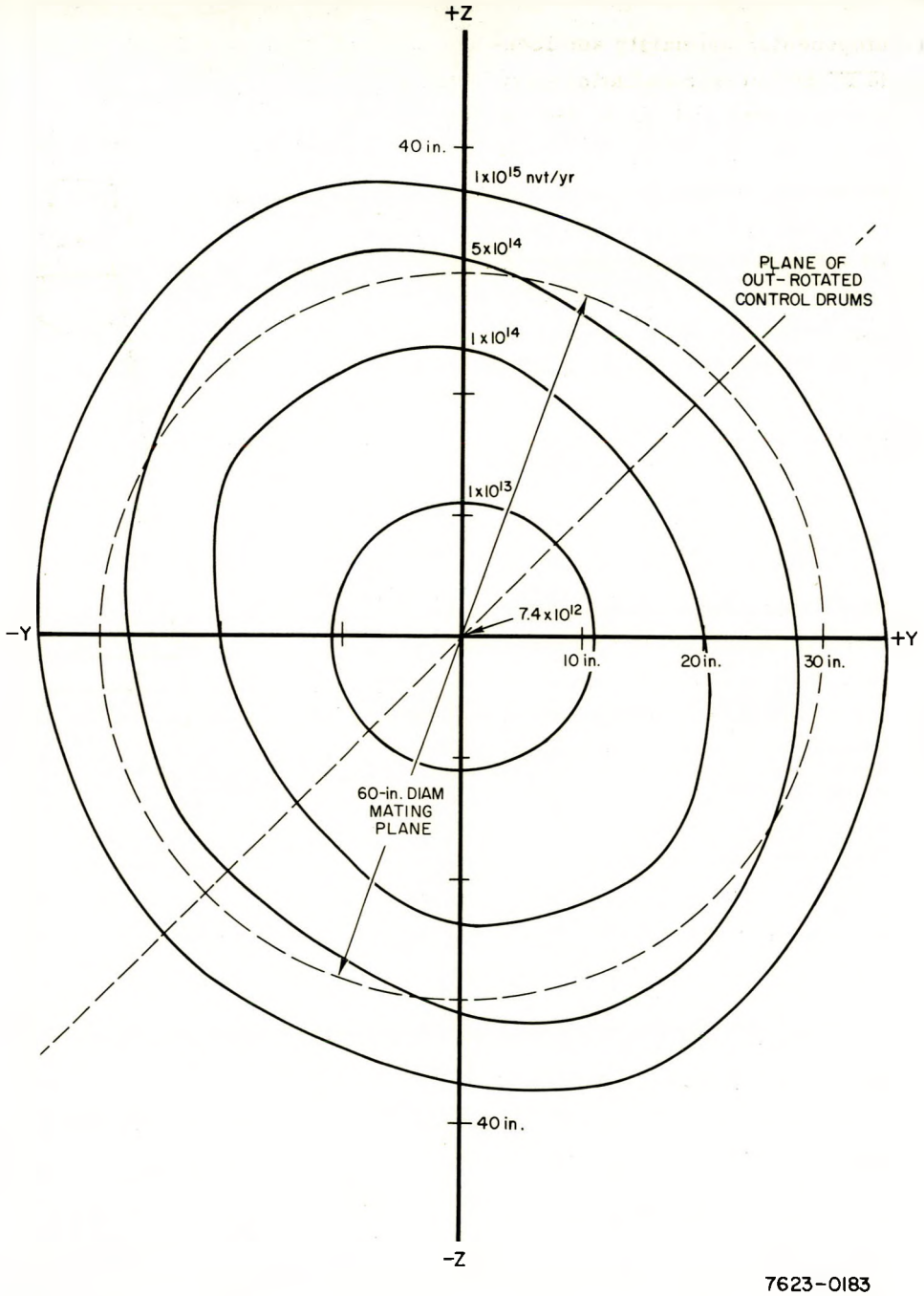

Figure 2. SNAP 10A Instrument Compartment Isoflux Map

II. SUMMARY OF RADIATION DAMAGE IN TRANSISTORS

Radiation damage of transistors is complex, and attempts at sophisticated analysis are frustrated by the disagreement between theory and experiment. In a reactor environment, fast neutrons are the predominant contributor to permanent transistor damage. Types of damage can be categorized into surface damage and bulk damage.

A. SURFACE DAMAGE

Conventional surface damage is caused by ionization of encapsulated gases and surface impurities which provide leakage paths at the surface of the transistor.[2] The damage generally can be recovered by removing either the transistor bias or the radiation field. Conventional surface damage usually reaches saturation at low radiation levels and the resulting degradation is small. However, serious degradation has been reported in isolated cases.[3] The first radiation-caused failure in Telstar at an equivalent neutron exposure of about 4×10^{11} nvt was surface damage. The damage was recovered by de-energizing the failed transistors.[4]

B. BULK DAMAGE

Radiation bulk damage refers to changes in the transistor structure which alters its electrical characteristics. Electrical conductivity, mobility of current carriers, the number of current carriers, and the minority carrier lifetime all change during irradiation. However, the first-order effect and the only one considered in this report is the decrease in minority carrier lifetime which results in the decrease of transistor gain.

C. DEGRADATION OF TRANSISTOR GAIN

The following expressions show the relationship between transistor current gain and fast neutron flux[5, 6]:

$$\frac{1}{\tau} = \frac{1}{\tau_o} + K\varphi \qquad \ldots (1)$$

$$\tau \approx \bar{t}\ h_{FE} \approx \frac{\bar{t}}{Q},\ Q < 0.1 \qquad \ldots (2)$$

$$K = \frac{dQ}{\bar{t}\, d\varphi} \qquad \ldots (3)$$

where:

φ = fast neutron flux, n/cm^2-sec,

h_{FE} = forward static current gain of the transistor,

$\bar{t}$ = minority carrier base transit time, sec,

$Q \approx \frac{1}{h_{FE}}$ = ratio of transit time to carrier lifetime, and

K = radiation damage constant for the material used, cm^2/n.

Algebraic manipulation of (1) and (2) yields the following correlation between the fast neutron flux and the normalized transistor gain:

$$\frac{h_{FE}}{h_{FE_o}} = \frac{1}{1 + K\bar{t}\, h_{FE_o}\varphi}$$

where

h_{FE_o} = initial nonirradiated transistor gain.

III. DETECTOR DEVELOPMENT

A. DETECTORS CONSIDERED

1. Conventional Instrumentation

Conventional fast neutron detection systems for the anticipated flux levels between 10^5 to 10^7 n/cm^2-sec would typically consist of a fission counter with a power supply and a pulse-counting system. The complexity and weight and space requirement prohibited the use of a series of conventional detection systems for this application.

2. Solid State Detectors

Both semiconductor diodes and transistors show promise as fast neutron sensors. During irradiation, the gain of a transistor decreases and the forward voltage drop of a diode increases. Both can be measured easily and correlated to the integrated flux. More information was available on transistor degradation, hence the major effort of this development used a transistor as the sensor.

As a backup effort, some radiation tests were conducted on a diode designed for fast neutron detection (Phylatron Type Ph-20). The test results were encouraging. However, development of the transistor detector was more advanced and appeared satisfactory, and the diode tests were discontinued.

B. TRANSISTOR SELECTION AND SCREENING

The existing literature was reviewed for a radiation-sensitive transistor with repeatable and predictable degradation characteristics in a fast neutron environment. It was anticipated from the literature that the concurrent thermal neutron and gamma fluxes would cause insignificant degradation of the transistor. Although degradation reports for transistors are plentiful, they are all slanted toward proving that the specific transistors are radiation-resistant. Thick base transistors are extremely radiation sensitive but the repeatability and predictability are very poor.

Developmental tests on small quantities of transistors started in the fall of 1962 indicated that the Texas Instruments 2N697 transistor exhibited repeatable and predictable degradation characterisitcs. One hundred of these transistors were procured and 60 were irradiated. Analysis of the irradiation data confirmed that the degradation characteristics of transistors with similar h_{FE}'s were repeatable. Also, the degradation could be predicted from the initial gain of the transistor.

The transistor tested, a Texas Instruments 2N697, is a high-speed medium-power NPN double-diffused planar silicon transistor with a current gain ranging from 40 to 120. To minimize variances due to dissimilar transistors, 400 transistors from the same manufacturing batch were procured. The 400 transistors were graded and 96 transistors with similar h_{FE}'s were selected for flight systems. The temperature coefficients of the 96 transistors were measured and the transistors with similar temperature coefficients were used on the flight system, and for calibration and qualification testing.

C. TEMPERATURE CONSIDERATIONS

1. Temperature Coefficient

The major temperature problem was the sensitivity of transistor gain to temperature. Temperature compensation of a nonirradiated transistor was relatively routine. However, it was not known if the temperature coefficient of a transistor remained constant during irradiation. It was decided to design temperature compensation for a nonirradiated transistor and determine if this compensation was adequate after irradiation.

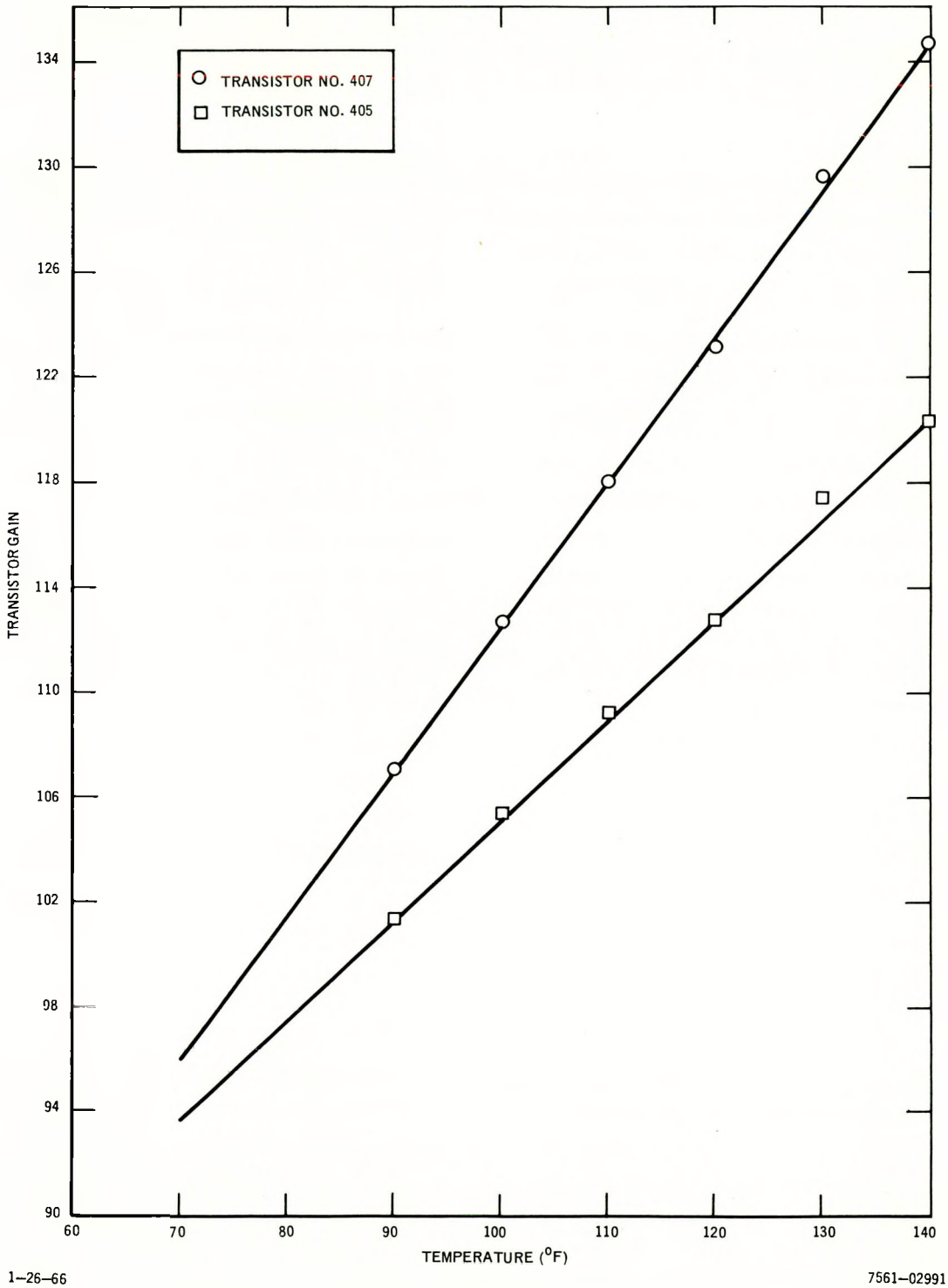

Figure 3. Temperature Coefficient Extremes

The measured temperature coefficients of 96 transistors selected as flight candidates were linear and similar with a few exceptions. The temperature coefficients of the eight flight detectors ranged from 0.37%/1 to 0.51%/1°F with an arithmetical mean of 0.41%/1°F. The two extreme temperature coefficients of the flight detectors are shown in Figure 3. The 40% change in gain for transistor No. 407 from 70 to 140°F emphasizes the need for temperature compensation.

The resistor-thermistor combination and the thermistor temperature coefficient required for the average temperature coefficient, and the planned collector current of the transistor were calculated. An assortment of thermistors bracketing the nominal calculated resistance and thermistor temperature coefficient were obtained.

Temperature cycling tests were conducted for various combinations of thermistors, resistors, and transistors. The selected thermistor-resistor combination is shown on Figure 4. Figure 5 shows the typical temperature sensitivity of a detector before and after compensation. Figure 5 also shows that the temperature compensation is not only adequate but also is much better for an irradiated detector.

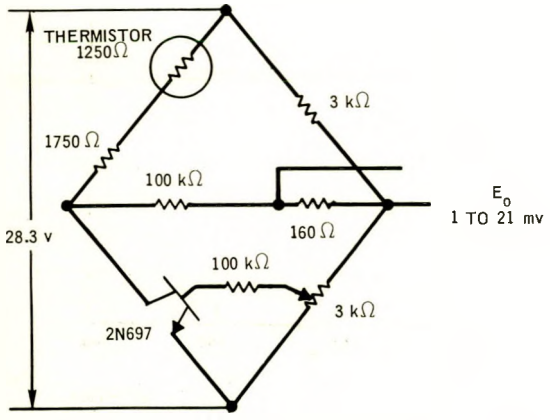

Figure 4. Detector Schematic

2. Transistor Stability and Annealing

The initial plan was to preirradiate the transistor sensors to some predetermined level beyond the damage threshold before installing them in the detectors. However, it was discovered that irradiated transistors annealed (recovered some of their gain) when continuously energized or subjected to temperatures above room ambient. Attempts to determine the annealing mechanism or means for minimizing annealing were unsuccessful.

A series of annealing tests was conducted on irradiated transistors using a common emitter circuit. Generally, a group of three similar transistors were operated at the predetermined temperature and base current which were kept constant for the duration of the test. The test durations ranged from 31 to 105 days. Most of the tests were conducted with one group at ambient and the other at 140°F. Base currents were set for initial collector currents ranging from 30 microamps to 5 milliamps. Transistors both energized and not energized during irradiation were tested.

The test results were inconclusive but the following qualitative observations were made:

1) No annealing was noted for highly irradiated transistors (5×10^{13} nvt) stored at room temperature for six months.

2) For transistors irradiated to the same level, annealing rate and degree of annealing was about the same when:

a) The transistors are not energized at 140°F.

b) The transistors are at room ambient or 140°F and energized with any collector current ranging from 0.04 ma to 5 ma.

3) The annealing rate was initially parabolic, then became linear with no saturation apparent after 104 days of continuous testing.

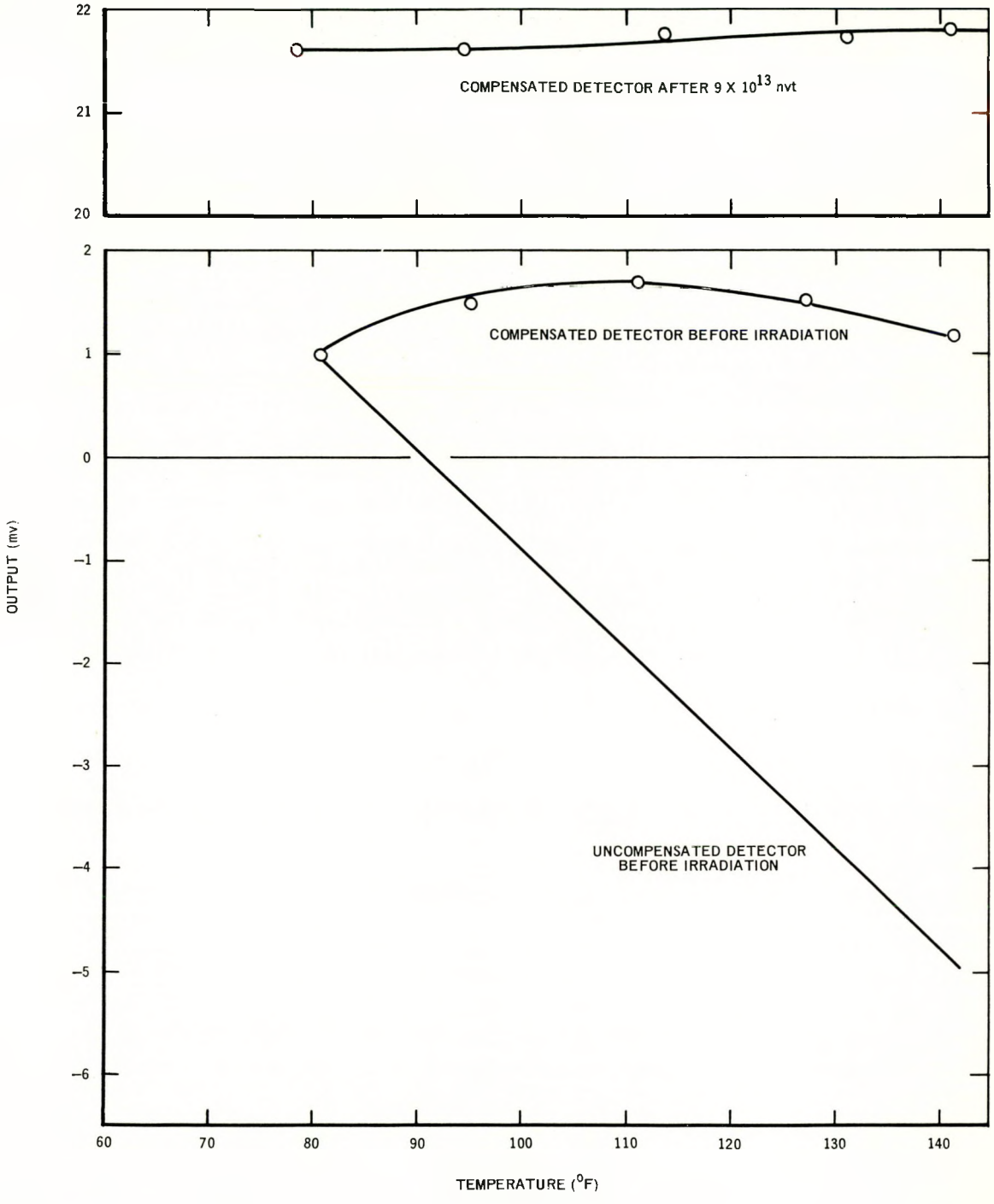

Figure 5. Temperature Compensation

4) Similar annealing rates and degrees of annealing were observed for transistors energized (active) during irradiation when compared with transistors not energized (passive) during irradiation.

It appeared that annealing could be related entirely to the collector-base junction temperature of the transistor. Heating the transistor would naturally heat this junction and the passage of current results in Joule heating (I^2R) of the junction. The collector-base junction temperature of a 2N697 transistor was determined using the method described in Reference 7. Measurements were made at 77°F and about 140°F using various collector currents. The results are shown in Table 1.

It was concluded that no direct correlation of annealing to collector-base junction temperature could be made since about the same annealing was observed at junction temperatures of 88 and 153°F.

To correlate degree of annealing with degree of irradiation, tests were conducted using transistors irradiated to 0, 1.6×10^{12}, and 5×10^{13} nvt. The family of curves shown in Figure 6 indicates very little annealing for transistors irradiated to 1.6×10^{12} nvt and considerable annealing at 5×10^{13} nvt. These tests were conducted at 140°F using a common emitter circuit with the collector current, I_c, held constant.

TABLE 1

JUNCTION TEMPERATURE VS I_c AND AMBIENT TEMPERATURE

Ambient Temperature (°F)	I_c (ma)	Junction Temperature (°F)	Junction Temperature Above Ambient (°F)
77	0	77	0
77	1	88	5
77	5	102	25
77	10	130	53
138	0	138	0
138	1	143	5
140	5	153	13
141	10	166	25

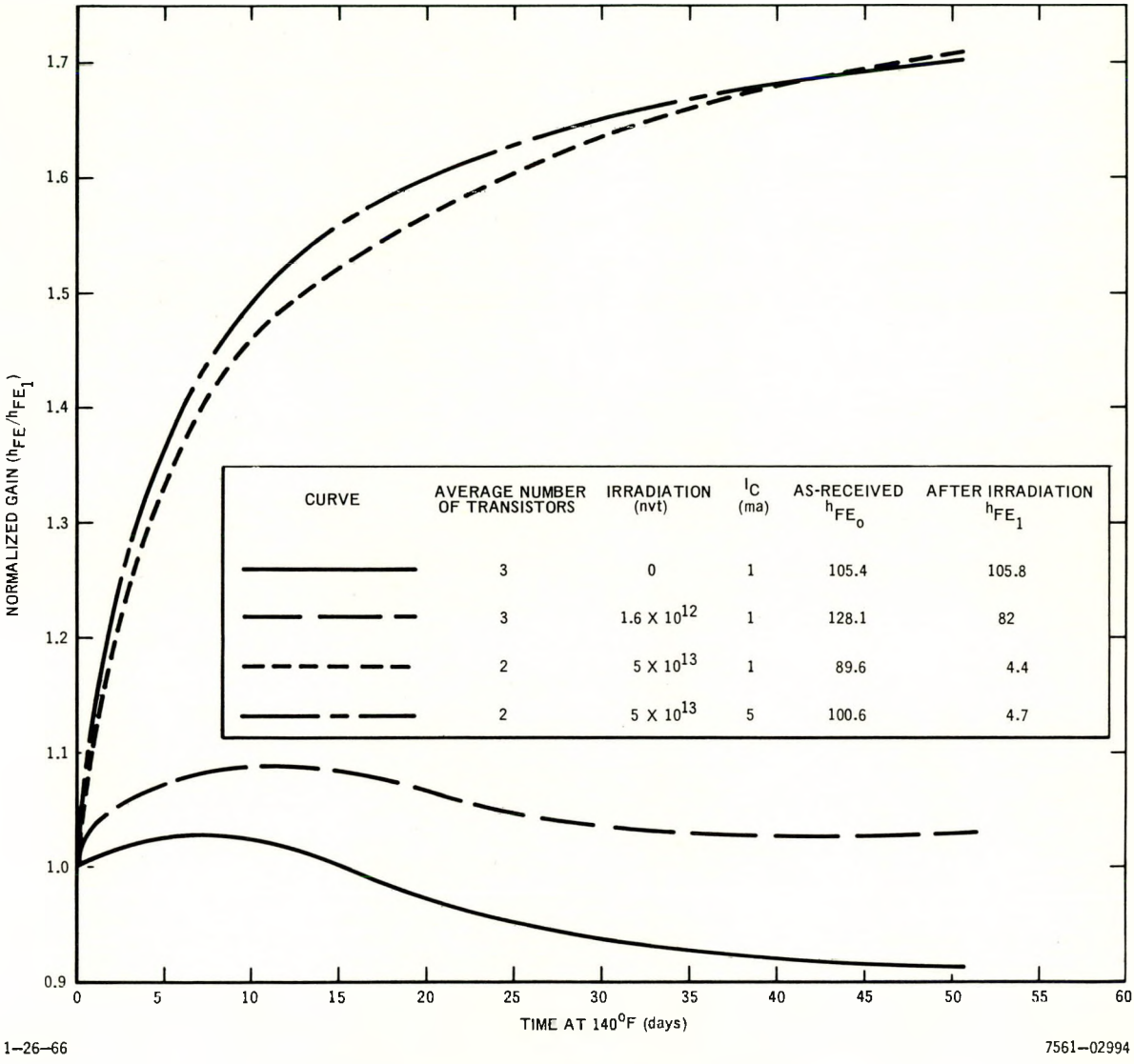

Figure 6. Annealing of Irradiated Transistors

IV. DETECTOR DESIGN AND FABRICATION

A. DESCRIPTION

The detector circuit consists of a bridge network with the transistor as the variable leg (Figure 4). A thermistor was used to compensate for variations of transistor gain due to temperature. The variable 3,000-ohm resistor was adjusted for an initial output of 1 mv. The 1- to 21-mv range of the detector corresponds to a degradation in normalized gain (h_{FE}/h_{FE_o}) from 1 to 0. The potted detector was 1 1/4 x 1 1/4 x 3/4 in. and weighed less than 3 oz with wiring. Each detector consumed 0.26 watts.

B. FABRICATION AND INSTALLATION

Thirty flight-type detectors were fabricated. Figure 7 shows one unpotted detector and one complete detector. Forty-eight developmental detectors were fabricated for SNAP 10A mockup and test systems.

The eight locations selected in the instrument compartment were a compromise between the desired locations for flux mapping and the availability of space, power, and mounting facilities. Figure 8 shows the detectors mounted in the instrument compartment.

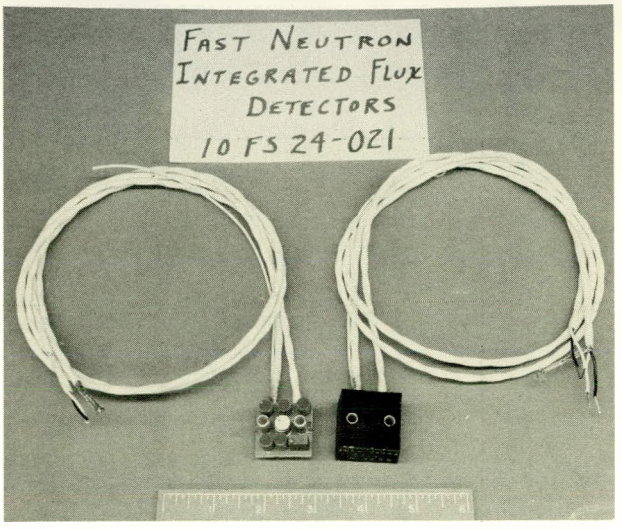

12-9-64 7561-551382

Figure 7. Unpotted Detector and Complete Detector

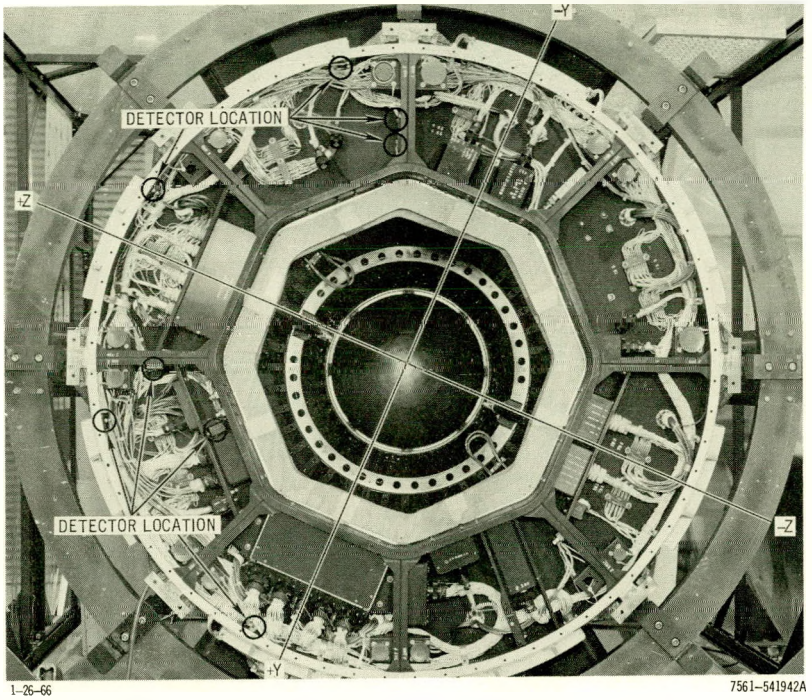

Figure 8. Location of Eight Detectors in the Instrument Compartment

V. RADIATION TESTING

A. GENERAL

Table 2 summarizes the radiation tests performed on selected transistors from the procured lot of 400. This table does not include earlier feasibility testing dating back to 1962 or the irradiation of 60 transistors referred to in III-B.

Test results indicate that the fast neutron response is repeatable and predictable but the gamma response is erratic.

The lithium hydride shield on SNAP 10A attenuates the fast neutron flux three decades but the gamma attenuation is insignificant. Therefore, the instrument compartment has a

TABLE 2
RADIATION TESTS ON SELECTED TRANSISTORS

Test Dates	Quantity Tested	Irradiation Facility	Total Flux Exposures	n/rad Ratio	A-Transistor Active (energized) During Irradiation P-Transistor Passive (de-energized) During Irradiation
9-14-64 to 10-11-64	54 Transistors	L77 Reactor	7.2×10^{11} nvt 4.3×10^{12} nvt 1.7×10^{13} nvt	10^8	A, 3 transistors in each of 18 combinations of temperature, flux rate, and initial transistor gain
11-18-64	6 Transistors	X-ray (150 kev)	5×10^5 rad		P, surface damage study
1-11-65	6 Detectors	STIR reactor fission plate	9×10^{13} nvt 5.8×10^5 rad	1.5×10^8	A, 120°F, detectors behind 2 in. of lithium hydride for neutron spectrum hardening
1-19-65 to 1-22-65	2 Detectors	2600 curie Co^{60} source	3×10^7 rad		A, ambient temperature
1-22-65	6 Transistors	2600 curie Co^{60} source	4×10^6 rad		P, ambient temperature
1-22-65 to 1-28-65	2 Detectors	2600 curie Co^{60} source	5.5×10^5 rad		A, ambient temperature
1-28-65 to 2-10-65	12 Transistors 3 Detectors	2600 curie Co^{60} source	6.5×10^5 rad		A, 6 transistors and 3 detectors, P, 6 transistors, ambient temperature
2-8-65	12 Transistors 3 Detectors	STIR reactor in pool	4.5×10^{12} nvt 3×10^6 rad	1.5×10^6	A, 6 transistors and 3 detectors, P, 6 transistors, 120°F
3-9-65 to 3-10-65	8 Transistors	STIR reactor in pool	2.2×10^{12} nvt 2.8×10^5 rad	8×10^6	A, 120°F

relatively low neutron/gamma ratio. The potential problem of gamma damage masking neutron damage was evaluated at the start of development and appeared to be non-existent. Hence, gamma tests were not included in the developmental testing. Qualification testing revealed that the gamma damage in the 2N697 transistor was as much as ten times greater than the maximum reported in literature.[8] The unexpectedly high gamma sensitivity of the detector and the low neutron/gamma ratio in the instrument compartment necessitated additional tests in a neutron-gamma environment similar to SNAP 10A. These tests indicated that gamma damage is significant and adversely affects the accuracy as shown in Table 3.

TABLE 3

ACCURACIES AT VARIOUS NEUTRON/GAMMA RATIOS

$\frac{n}{rad}$	Detector Accuracy at Midscale
10^8	±15%
8×10^6	±50%
1.5×10^6	Extremely Poor

Due to the unpredictable scatter in gamma damage data, a simple subtraction of gamma damage from total damage to determine fast neutron damage is not feasible.

B. PREDOMINANT FAST NEUTRON ENVIRONMENT TESTS

1. L77 Reactor Irradiation

Fifty-four transistors were irradiated in AI's L77 reactor. The L77 is a 10-watt homogeneous solution-type reactor using aqueous uranyl sulfate enriched to about 20% of U^{235} as the fuel in a 15-3/4-in. diameter spherical core. The core and a three-region shield are located in a water-filled cylindrical shield tank 8 ft in diameter by 7 ft high (Figure 9). The transistors were tested on fixtures installed in the two beam tubes. Figure 10 shows the outside of the reactor shield tank, one test fixture

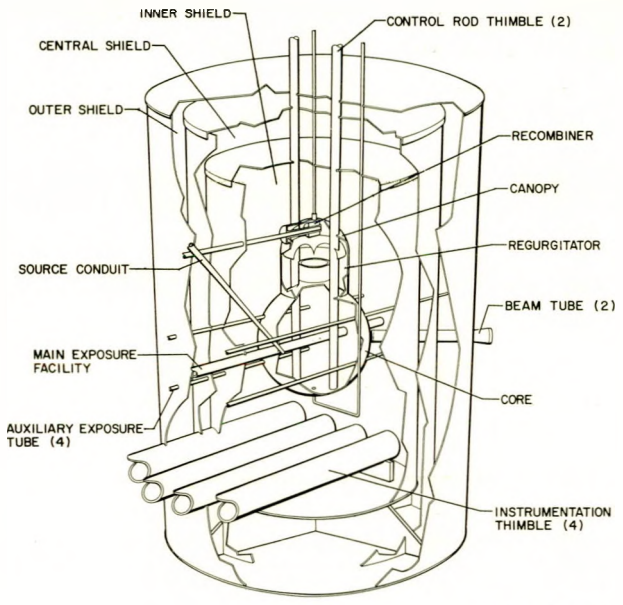

7561-02995

Figure 9. L-77 Reactor

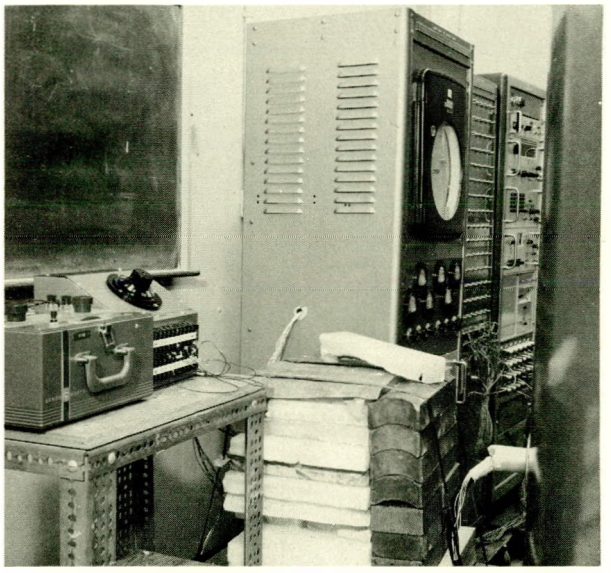

9-16-64 7561-18526

Figure 10. L-77 Test Setup

inserted in a beam tube, and the test instrumentation. Common emitter circuits were used for all transistors. The base current was set for an initial collector current of 4.6 ma. The reactor was operated at 3.3 watts 24 hours a day, 5 days a week for 4 weeks. The transistors were energized continuously for the 4 weeks.

The purpose of the L77 test was to determine if detector response was affected by variations in temperature, flux rate, and initial transistor gain. The ranges of the variables expected in SNAP 10A are shown in Table 4. The 54 transistors were irradiated, 3 in each of the 18 possible combinations of the variables shown in Table 4.

TABLE 4
L77 TEST CONDITIONS

Temperature (°F)	Flux Rates (n/cm^2-sec)	Initial Transistor Current Gain
110	5×10^5	43
130	3×10^6	72
	10^7	117

The results of the test indicated that detector response is relatively independent of temperature, flux rate, and initial transistor gain. Detector sensitivity increases with increasing flux rate, initial transistor gain, and decreasing temperature; however, this dependence is weak. The spread of the response curve for three similar transistors operating at the same flux rate and temperature generally overrides the effects of varying temperature, flux rate, and initial transistor gain.

2. STIR Fission Plate Irradiation

Six detectors similar to the ones used on the SNAP 10A FS-4 flight system were irradiated at the fission plate of the Shield Test and Irradiation Reactor (STIR). STIR is a 1-Mw pool-type reactor with facilities for irradiation in the pool and in the shield test room (Figure 11). One wall of the shield test room contains a graphite thermal column adjacent to the reactor core. A highly enriched U^{235} fission plate can be driven from its cask to a position adjacent to the thermal column.

The purpose of the STIR irradiation was to obtain calibration data which could be used to interpret the flight data. The fast neutron spectrum in SNAP 10A was simulated by mounting the detectors behind 2 inches of lithium hydride. The test temperature was 120°F. After 29 hours of continuous irradiation the integrated flux at the detectors was 9×10^{13} nvt. The flux rate was progressively increased from 1.66×10^7 to 2.44×10^9 n/cm^2-sec. Figure 12 shows the response envelope for the six detectors.

Before the STIR calibration, the response was predicted from the relationship

$$\frac{h_{FE}}{h_{FE_o}} = \frac{1}{1 + K\bar{t}h_{FE_o}\varphi} .$$

An average damage constant, K, was calculated from the L77 irradiation. The preirradiation gain, h_{FE_o}, and the base transit time, $\bar{t}$, were measured. The agreement between the predicted and measured responses was good. Figure 13 shows the poorest agreement between predicted and measured response for the six transistors.

For similar transistors, the widest variation of the transistor constants, K, $\bar{t}$, and h_{FE_o}, was in the damage constant K. Results of the L77 irradiation indicated that K variations of 20% were common for similar transistors operating at the same temperature, flux rate, and current. Since K cannot be measured without destroying the transistor, improving

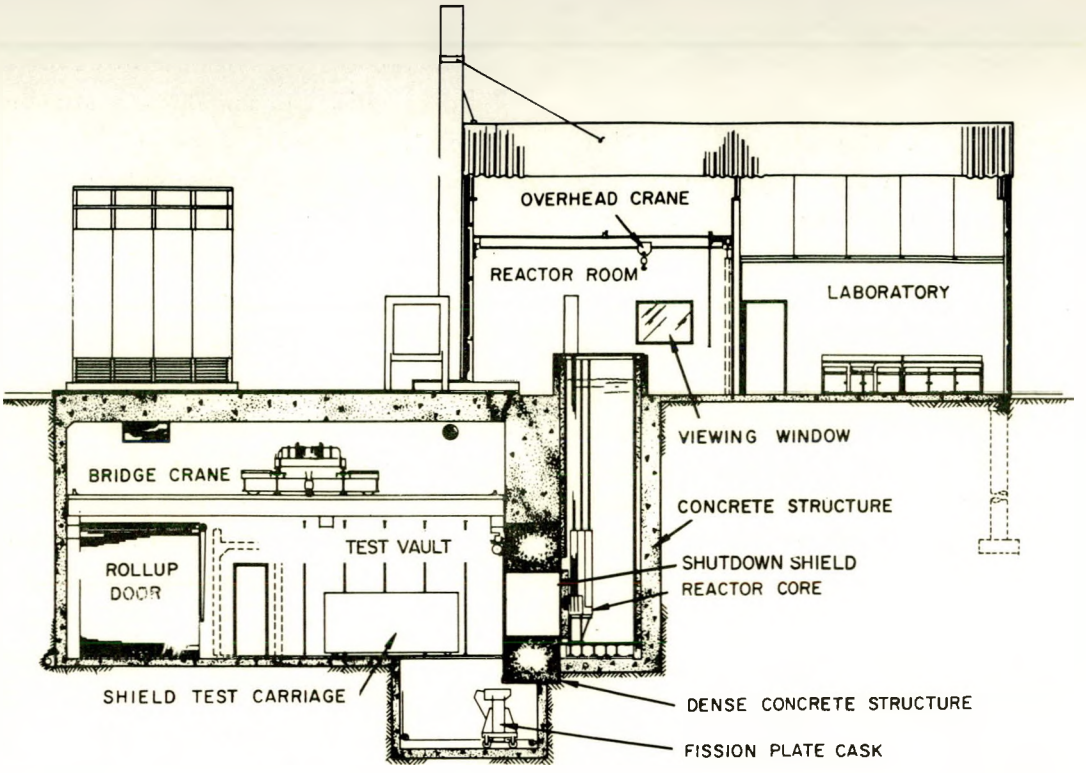

Figure 11. STIR Facility

the accuracy of the predicted response is not feasible.

C. X-RAY TESTS

X-rays were used to determine the extent of surface damage on the 2N697 transistors. Five transistors were exposed to 5×10^5 rad. Figure 14 shows that the surface damage on 2N697's is erratic but appreciable, and gain has degraded to about 70% of initial gain at relatively low doses of 1 to 3×10^5 rad.

Generally, surface effects can be recovered by removing the transistor bias or by removing the irradiating source (Reference 2). Contrary to this general behavior of transistors, the surface effect of the 2N697's could not be recovered using these normal methods.

D. GAMMA ENVIRONMENT TESTS

The detector's exposure to gamma irradiation started as a routine part of the qualification tests. Literature[8,9] indicated that transistor damage would be due predominantly to fast neutrons.

Gamma damage is not as predictable or repeatable as neutron damage; consequently, experimental efforts to determine a neutron/gamma damage equivalence have resulted in the wide range of reported equivalences shown in Table 5.[8,9]

TABLE 5
NEUTRON DAMAGE EQUIVALENCE (n/cm^2) OF ONE-RAD

Lowest	Most Probable	Highest
4.82×10^4	5.2×10^5	2.5×10^6

Table 6 shows the calculated percentages of gamma damage to total damage for each detector based on the calculated neutron and gamma

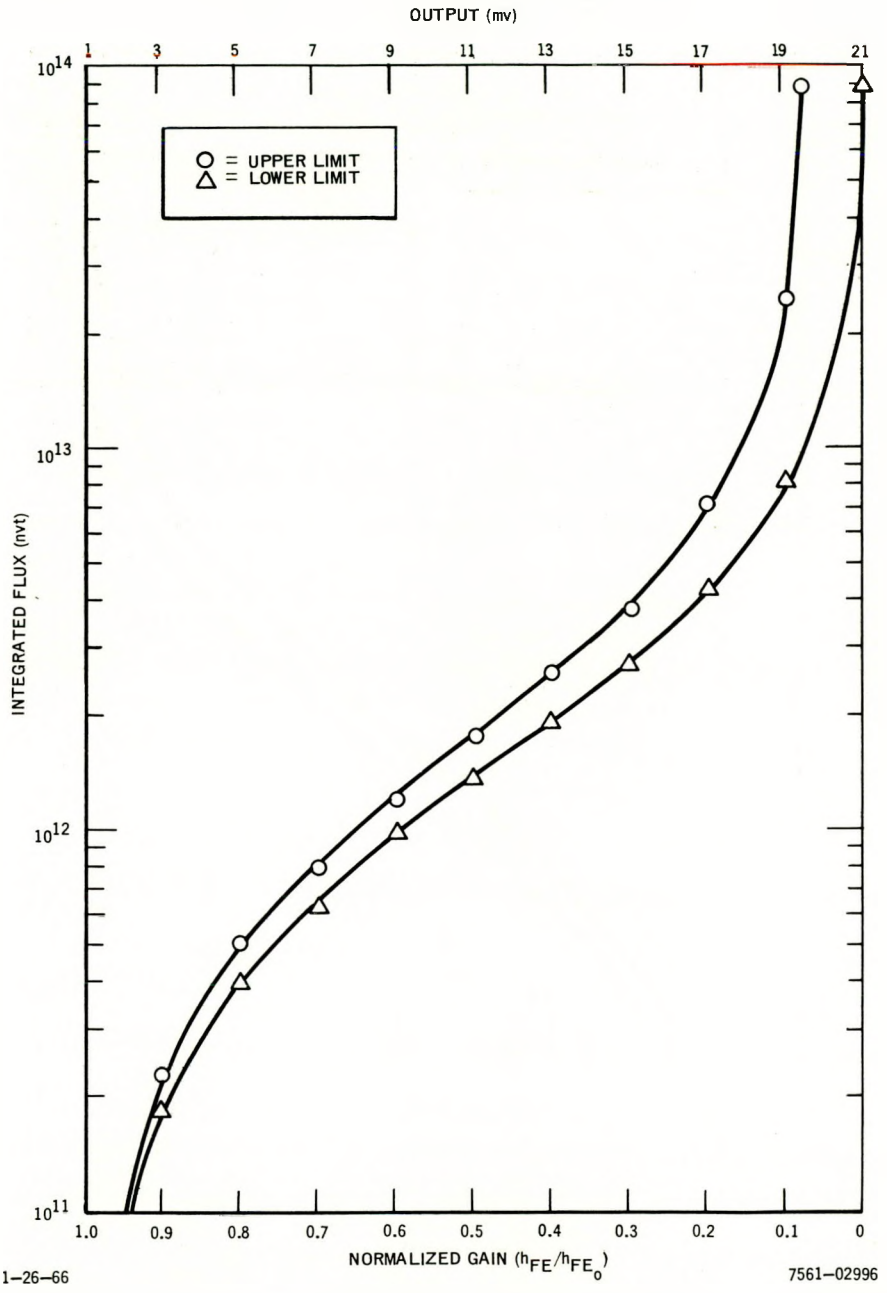

Figure 12. STIR Calibration Response Envelope at 1.5 x 10^8 n/rad

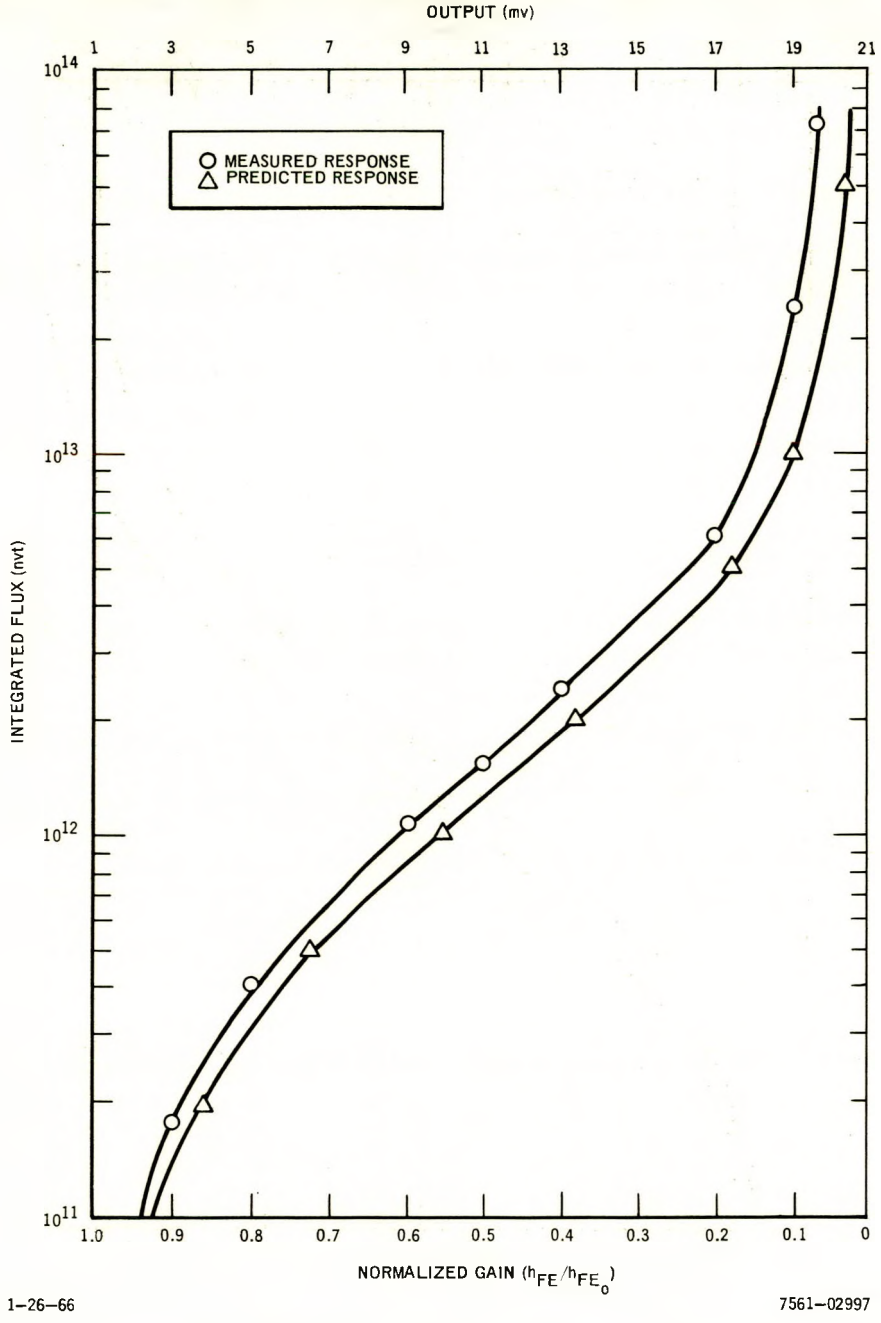

Figure 13. Measured Response vs Predicted Response

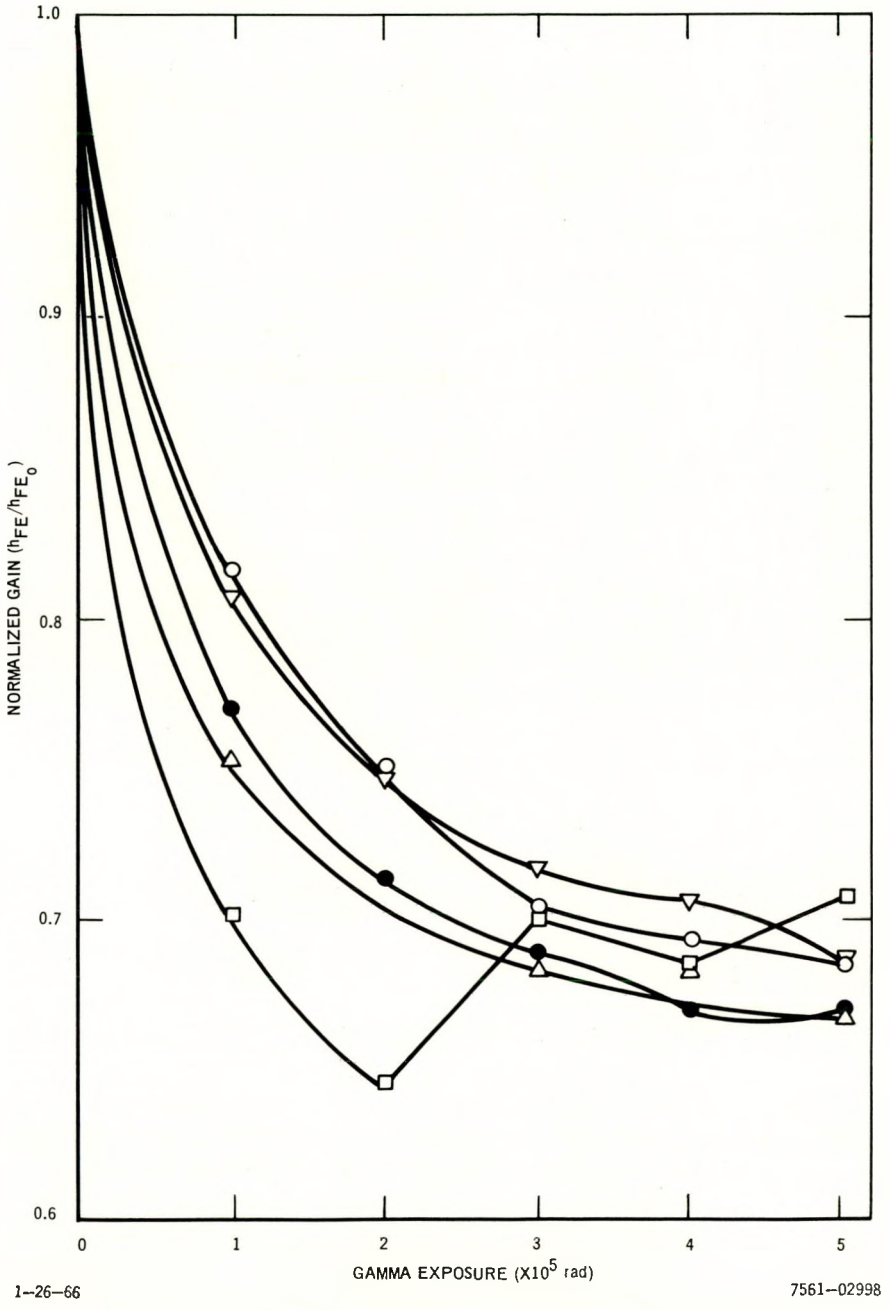

Figure 14. Transistor Surface Damage on Five 2N697's

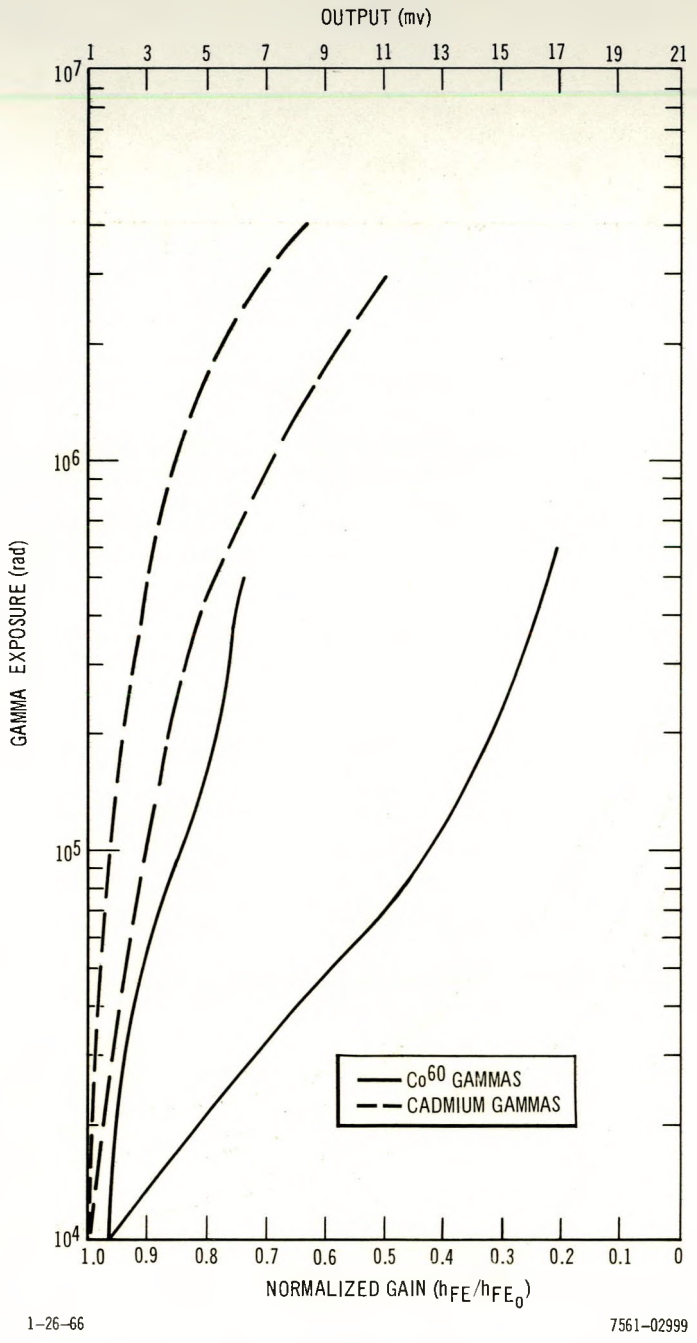

Figure 15. Gamma Response of Detectors

TABLE 6

PERCENT OF GAMMA DAMAGE TO TOTAL DAMAGE

Detector	ND-1	ND-2	ND-3	ND-4	ND-5	ND-6	ND-7	ND-8
Most Probable (%)	2	2	6	20	2	5	12	12
Worst Case (%)	9	7	24	55	8	21	39	41

TABLE 7

CALCULATED n/rad RATIOS

Detector	ND-1	ND-2	ND-3	ND-4	ND-5	ND-6	ND-7	ND-8
n/rad x 10^6	24.7	31.7	7.8	2.07	27.1	9.5	3.87	3.65

fluxes at each detector and the reported most probable and worst case neutron/gamma damage equivalences.

The first gamma exposure of the detectors indicated high gamma sensitivity. Subsequent tests indicated that the 2N697 transistors were from 1.4 to 10 times more gamma sensitive than the worst case previously reported and from 7 to 44 times more sensitive than the most probable.

As previously noted, degradation of similar transistors due to fast neutrons was repeatable and predictable (Figures 12 and 13). In contrast, gamma degradation data for similar transistors exhibited considerable scatter and was not predictable (Figure 15). The solid lines in Figure 15 shows the response envelope for 28 transistors and detectors to Co^{60} gammas. The broken lines show the response envelope for four transistors to a higher-energy cadmium gamma spectrum. Contrary to the anticipated results, the higher-energy cadmium gammas appear less damaging than the lower-energy Co^{60} gammas. However, the results are inconclusive due to the differences in test conditions. The tests from which the solid lines were generated were at ambient temperature and used a common emitter circuit similar to the one shown in Figure 4 where I_b was held constant and I_c initially was 4.6 ma and decreased as the transistor degraded. Also, the tests from which the broken lines were generated were at 140°F and used a common emitter circuit but I_b was varied to maintain a constant I_c of 10 ma.

The electrical characteristics of the resistors and thermistor in the detector were monitored in one Co^{60} test to confirm that they suffered no degradation.

E. SIMULATED SNAP 10A ENVIRONMENT TESTS

Table 7 shows the calculated n/rad ratios at the eight detectors from the calculated neutron and gamma fluxes.

The response of the detectors in a neutron/gamma ratio lower than the SNAP 10A worst case (ND-4) was determined. Twelve transistors and three detectors were irradiated to 4.5×10^{12} nvt in the pool of the STIR reactor at 1.5×10^6 n/rad. The unbroken lines in Figure 16 show the envelope of the responses for six transistors and three detectors. Gamma degradation is manifested by the large degree of scatter and non-repeatability of the response curves.

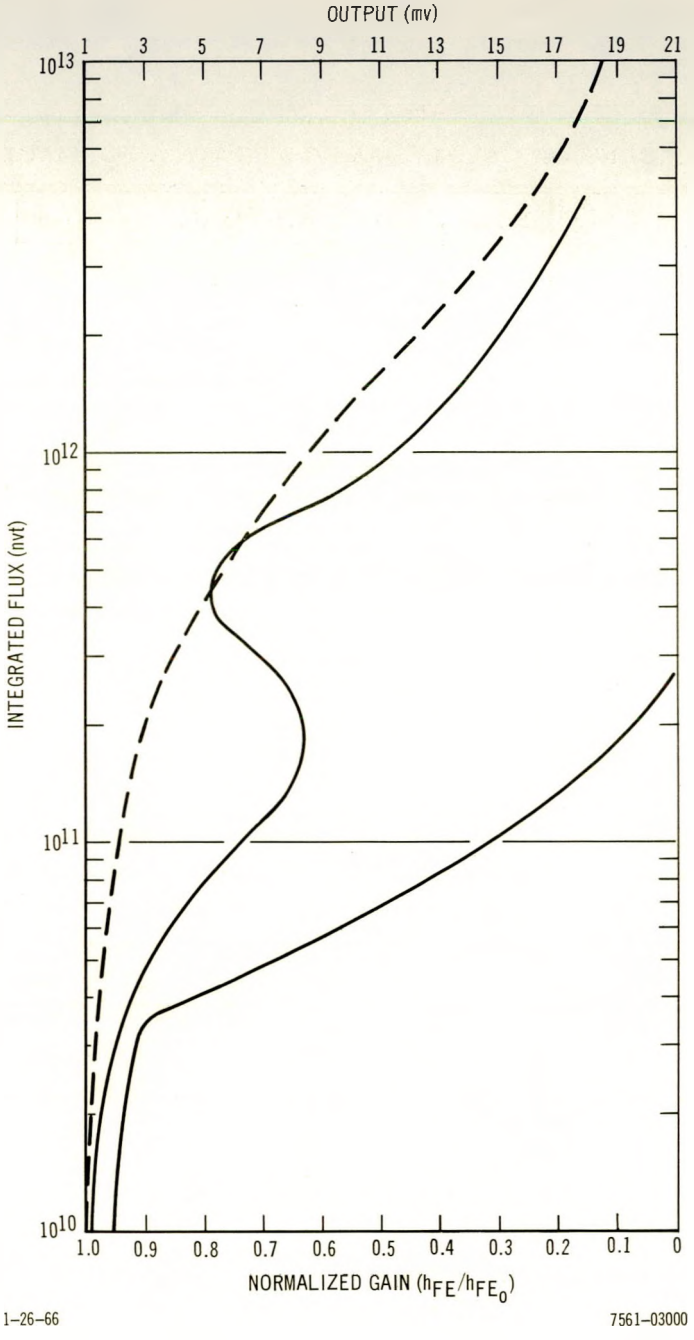

Figure 16. Detector Response Envelope at 1.5×10^6 n/rad

For comparison, the broken line in Figure 16 shows the average of the repeatable and predictable response at 1.5×10^8 n/rad (Figures 12 and 13). Obviously at 1.5×10^6 n/rad detector accuracy is extremely poor.

Since data indicated good accuracy (±15% at midscale) at 10^8 n/rad but extremely poor accuracy at 1.5×10^6 n/rad the next test was at 8×10^6 n/rad. Eight transistors were irradiated in the pool of the STIR reactor to 10^{13} nvt at 8×10^6 n/rad. The characteristic scatter of gamma degradation again was present in the response curves envelope (Figure 17). The response at 8×10^6 n/rad was not as erratic as the response at 1.5×10^6 n/rad. The spread at midscale, referred to an average curve, was about ±50%. One additional limitation at 8×10^6 n/rad was the scatter and extremely poor accuracy at low levels of irradiation.

F. NEUTRON SPECTRA UNCERTAINTIES

No attempt has been made in this report to correlate transistor degradation to neutron spectra. All dosimetry was normalized to a fission spectrum including the STIR in pool tests where the spectra of both tests were harder than a fission spectrum. For in-pool tests, the neutron spectrum hardens as the n/rad ratio decreases.[10] It was never proven that the additional degradation at lower n/rad ratios was due to gammas. The concurrent hardened neutron spectrum could cause the additional degradation. A test-proven correlation of transistor degradation to neutron spectra is not available; however, using vacancy formation theory, degradation is not a strong function of neutron energy at the higher energies.[11] In addition, the detector's extreme sensitivity to Co^{60} gammas indicate the gammas and not the harder spectrum are responsible for the added degradation at lower n/rad ratios.

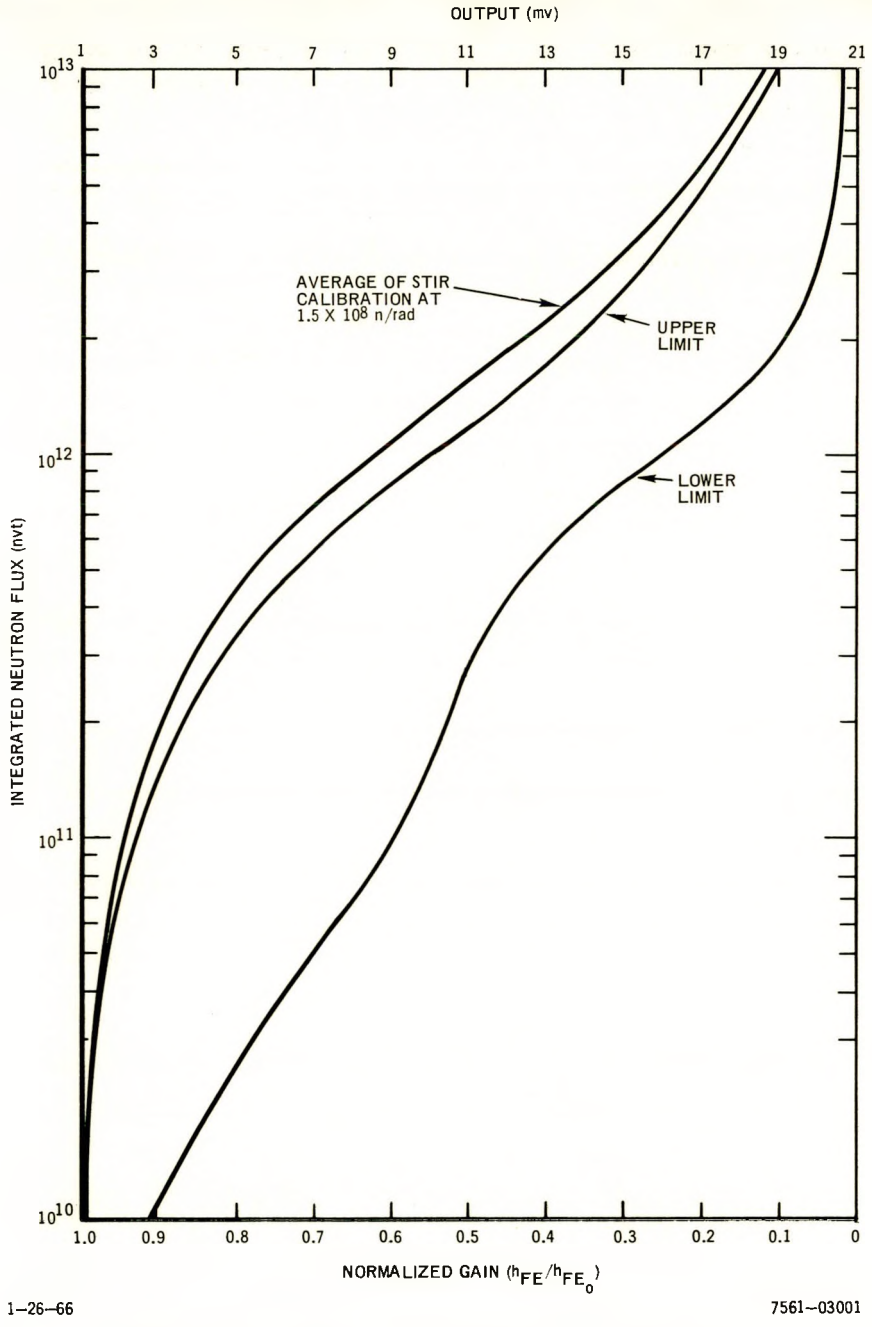

Figure 17. Detector Response at 8 x 10^6 n/rad

VI. QUALIFICATION TESTING

In addition to the radiation environment tests described, the detectors were flight qualified by test for the SNAP 10A launch and space thermal vacuum environments. Table 8 summarizes the test results.

TABLE 8
DETECTOR QUALIFICATION TESTS

Type Test	Quantity Tested	Incidents or Failures
Performance Record	19	0
Humidity	4	0
Temperature Stability	10	4*
Post Environmental Tests	4	0

*The deviations from the specification for these four devices were marginal.

VII. FLIGHT DATA

A. MALFUNCTION OF ONE DETECTOR

No in-flight data was received from ND-1. From the prelaunch data, it appears that the output polarity of the telemetry signal was inverted probably due to a wiring error.

B. GAMMA DATA

Gamma flight data indicated a relatively uniform gamma flux varying from 650 rad/hr to 716 rad/hr across the instrument compartment.

C. SOLID STATE DETECTOR DATA

The initial data from the solid state detectors were erratic indicating that gamma damage was present. To interpret the flight data, the method detailed in the Appendix was used. This method utilizes the slopes of the detector response curves between 13- and 17-mv output and attempts to separate neutron damage from the total damage. Since the accuracy of the detectors depends on the n/rad ratio at the detector, the upper and lower limits of flux rate were determined for each detector.

The basic information used for flight data interpretation is from the off-line steady state data generated by the FLAP 4 computer code. Each point is the average of all readings for that point during one pass of the SNAP 10A-Agena vehicle over one tracking station. The millivolt reading is converted to nvt by FLAP 4 using the average response curve at 1.5×10^8 n/rad.

Figures 18 and 19 show the output from FLAP 4 in the vicinity of the 13- to 17-mv range used for data reduction. For each detector, a least squares fit was used between 13 and 17 mv to determine the total equivalent flux rate which includes neutron and gamma damage. From this total equivalent flux rate,

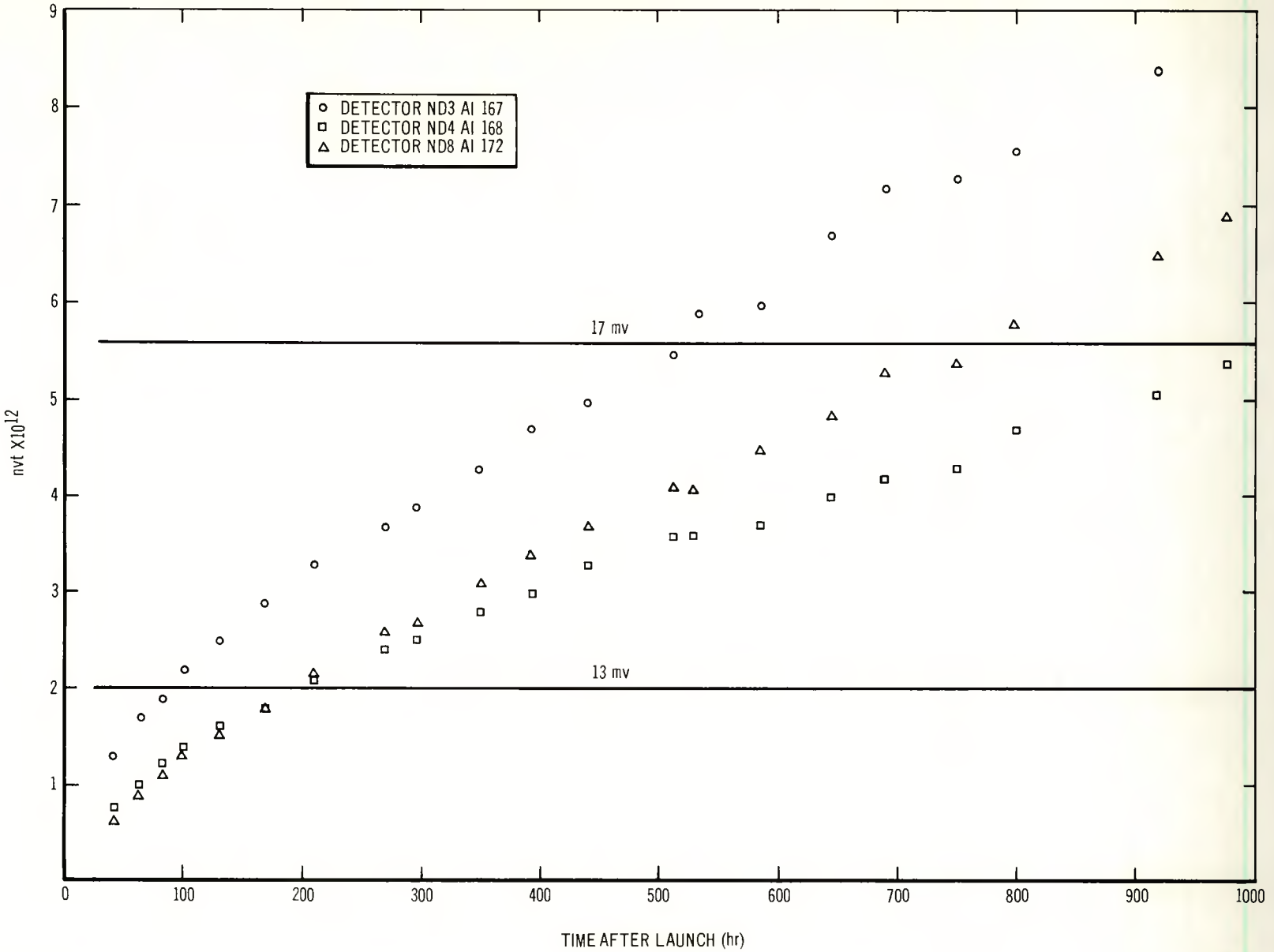

1-26-66

7561-03002-1

Figure 18. FS-4 Flight Data

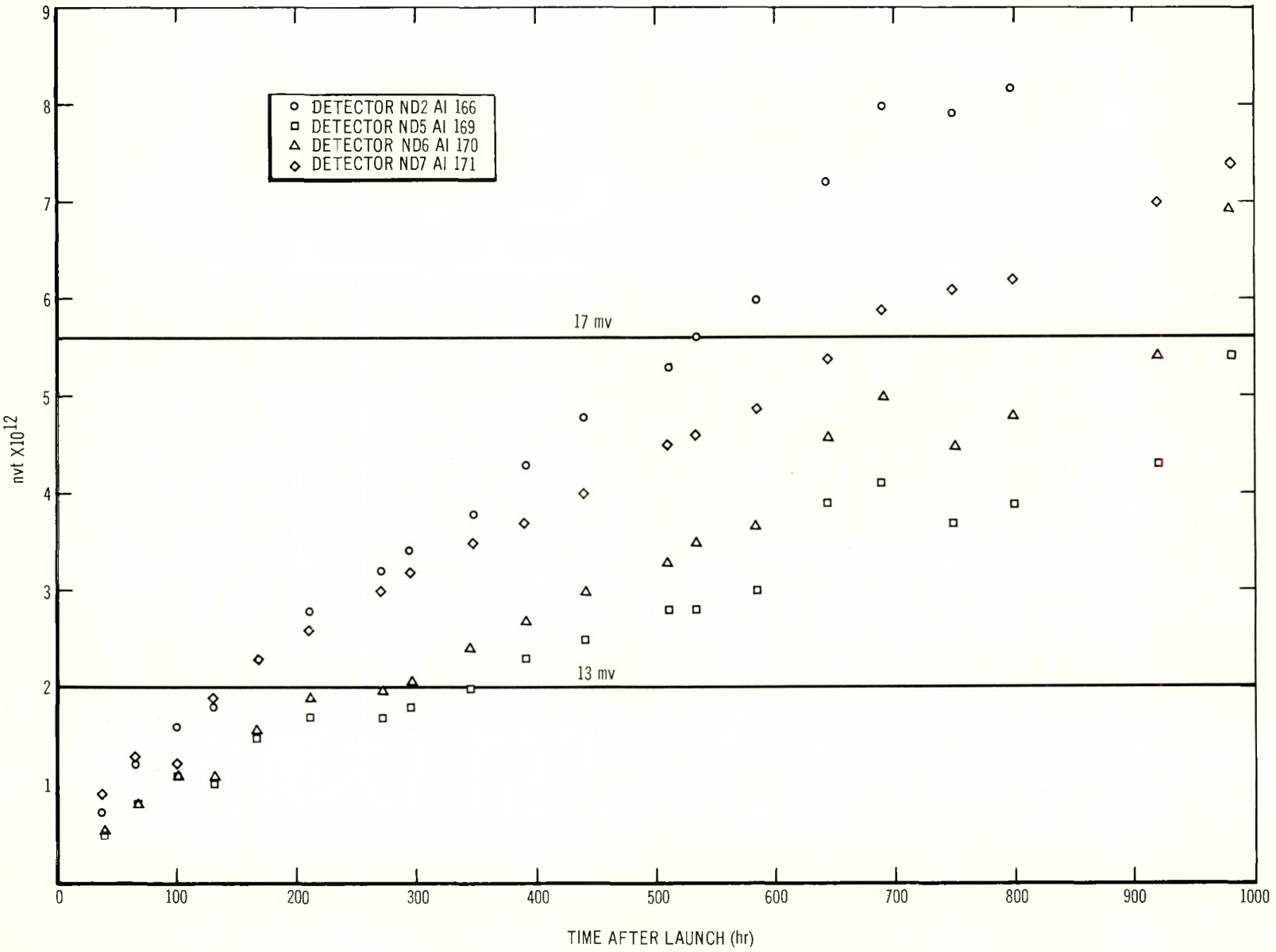

1-26-66

7561-03002-2

Figure 19. FS-4 Flight Data

SUMMARY OF DETECTOR EXPOSURES

Detector	$n + \gamma$ Equivalent Flux ($\times 10^6$)	Probable n Flux ($nv \times 10^6$)	Upper and Lower Limits on n Flux ($nv \times 10^6$)	$\frac{n^*}{rad}$ Ratio ($\times 10^6$)	Integrated Exposures 43 Days ($nvt \times 10^{12}$)	One Year ($nvt \times 10^{13}$)
ND 2	2.53	1.82	2.4 - 1.1	10	6.8	5.7
ND 3	2.28	1.58	2.1 - 0.96	8.7	5.9	5.0
ND 4	1.17	0.64	1.0 - 0.23	3.5	2.4	2.0
ND 5	1.30	0.73	1.1 - 0.32	4.0	2.7	2.3
ND 6	1.55	0.94	1.4 - 0.46	5.2	3.5	3.0
ND 7	1.75	1.10	1.6 - 0.57	6.1	4.1	3.5
ND 8	1.71	1.08	1.5 - 0.54	6.0	4.0	3.4

*Based on the measured gamma flux of 650 rad/hr

the calculated gamma damage was subtracted using the technique described in the Appendix.

Table 9 summarizes the calculated flux rates, the upper and lower limits on the flux rates, the integrated exposures for 43 days, and the extrapolated exposures for one year.

D. COMPARISON OF AI AND LMSC DATA

Both Lockheed Missiles and Space Company (LMSC) and Atomics International monitored the fast neutron and gamma fluxes near the SNAP 10A-Agena interface.

The AI gamma detector consisted of a 347 stainless steel walled ionization chamber backfilled with three atmospheres of nitrogen mated to a single-decade linear output signal conditioner. The LMSC gamma detectors employed a Bragg-Gray aluminum-walled carbon-dioxide-filled ionization chamber mated to a three-decade logarithmic output signal conditioner.

The LMSC fast neutron (>0.65 Mev) detectors utilized a cadmium-covered neptunium 237 fission chamber mated to a three-decade logarithmic output signal conditioner.

Figure 20 shows the fast neutron and gamma fluxes measured near the interface by AI and LMSC. Generally, good agreement exists considering the differences in the hardware used.

The largest inconsistencies are in the fast neutron fluxes which probably are the result of some combination of the following factors:

1) The dependence of the AI solid state detectors on neutron spectrum is unknown.

2) The main contributions to the fast neutron fluxes in the instrument compartment are direct penetration of the shield (hard spectrum) and scatter from the control drum projections and the converter (fission spectrum). It is expected that neutron spectra as well as neutron fluxes vary across the instrument compartment.

3) Neptunium 237 chambers are extremely sensitive to high-energy neutrons (>6 Mev) where the fission cross section increases rapidly with neutron energy.[11] They are also sensitive to gammas due to photofissions and to thermal neutrons due to the high impurity content of plutonium and uranium in neptunium.[12] During lithium hydride shielding experiments at AI, neptunium 237 chambers consistently indicated a higher flux than Hurst chambers of the same geometry in the same location.[12]

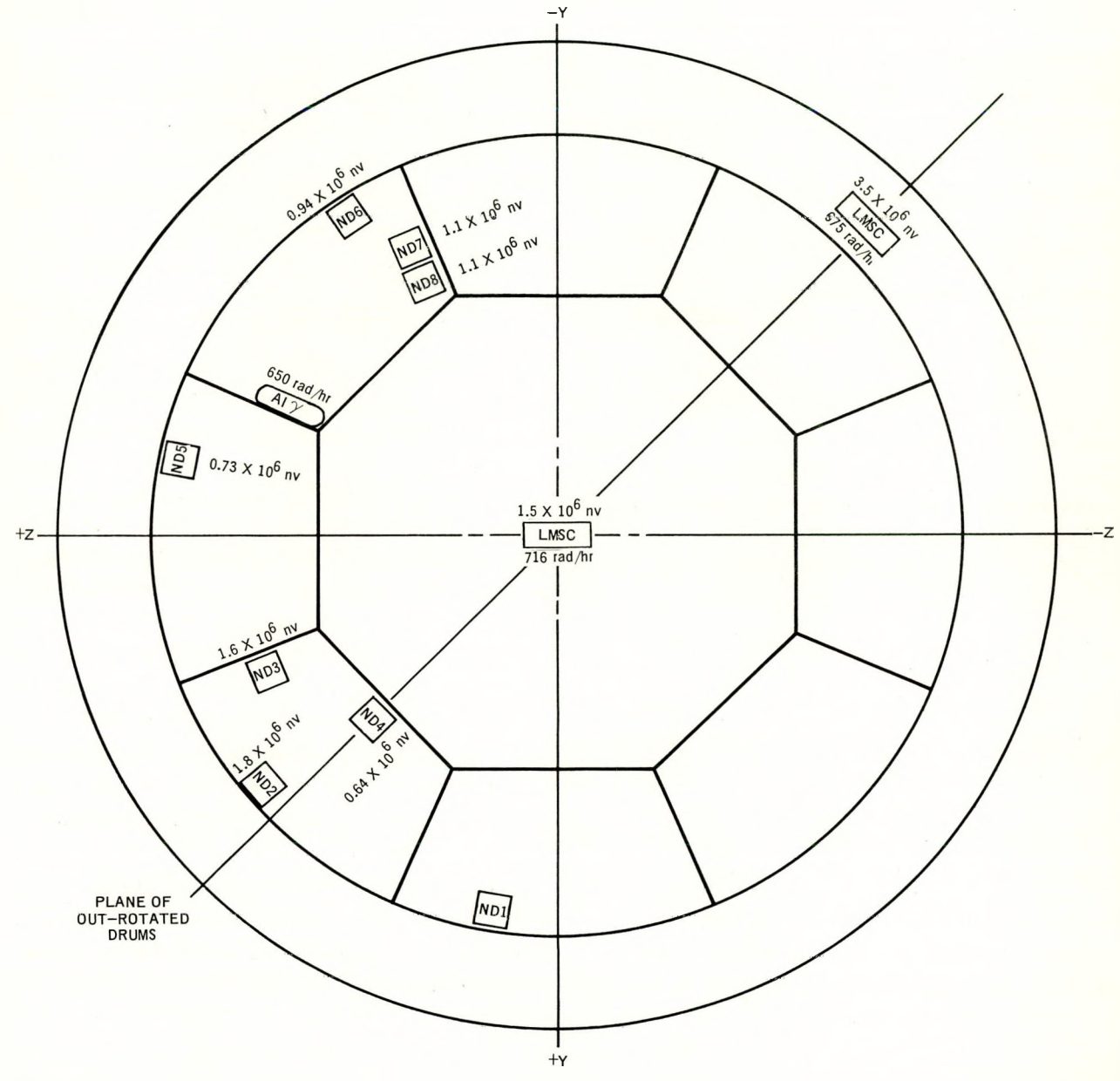

Figure 20. Measured Fast Neutron and Gamma Fluxes

VIII. CONCLUSIONS AND RECOMMENDATIONS

A. CONCLUSIONS

During development, it was proven by test that the detector response to fast neutrons is reasonably predictable and repeatable. The tests also proved that the response is relatively independent of flux rate, operating temperature, and initial transistor gain. Unfortunately, the first generation detectors were extremely gamma sensitive which decreased their accuracy and required an awkward method of data reduction to interpret the data.

B. RECOMMENDATIONS

For future testing the following recommendations are made:

1) Consider using a silicon diode as a sensor if it can be proven that they are insensitive to gammas. Preliminary fast neutron irradiation tests of silicon diode fast neutron detectors made by Phylatron indicated a high degree of repeatability. In addition, higher sensitivity without sacrificing predictability and repeatability appears feasible. The higher sensitivity is desirable since the trend seems to be toward lower radiation levels at the payload. One potential problem is that the diode temperature coefficient varies during irradiation.

2) For a transistor sensor, replace the Texas Instrument 2N697 transistor with a transistor less sensitive to gammas. Preliminary tests in a Co^{60} source indicate that the Fairchild 2N1613 may satisfy the requirement.

3) For a transistor sensor, the present constant-base current circuit should be changed to a constant-collector current circuit. Transistor current gain is a relatively strong function of collector current. A decrease in collector current results in a decrease in current gain. In the common emitter circuit used, the collector current decreases from 4.7 ma to 0 during irradiation. Degradation of gain during irradiation is compounded since a decrease in gain due to irradiation decreases the collector current which further decreases the gain.

The current-gain collector-current (h_{FE} - I_c) relationship varies among similar nonirradiated transistors. A much greater variation is noted for irradiated transistors with a strong dependence on the type of radiation. Gammas distort this h_{FE} - I_c relationship considerably. Figure 21 shows the average h_{FE} - I_c characteristics for similar transistors, nonirradiated, neutron irradiated, and gamma irradiated. Using a constant-current circuit will eliminate most of the variations noted in Figure 21 and probably improve the predictability and repeatability of transistor degradation in a radiation environment.

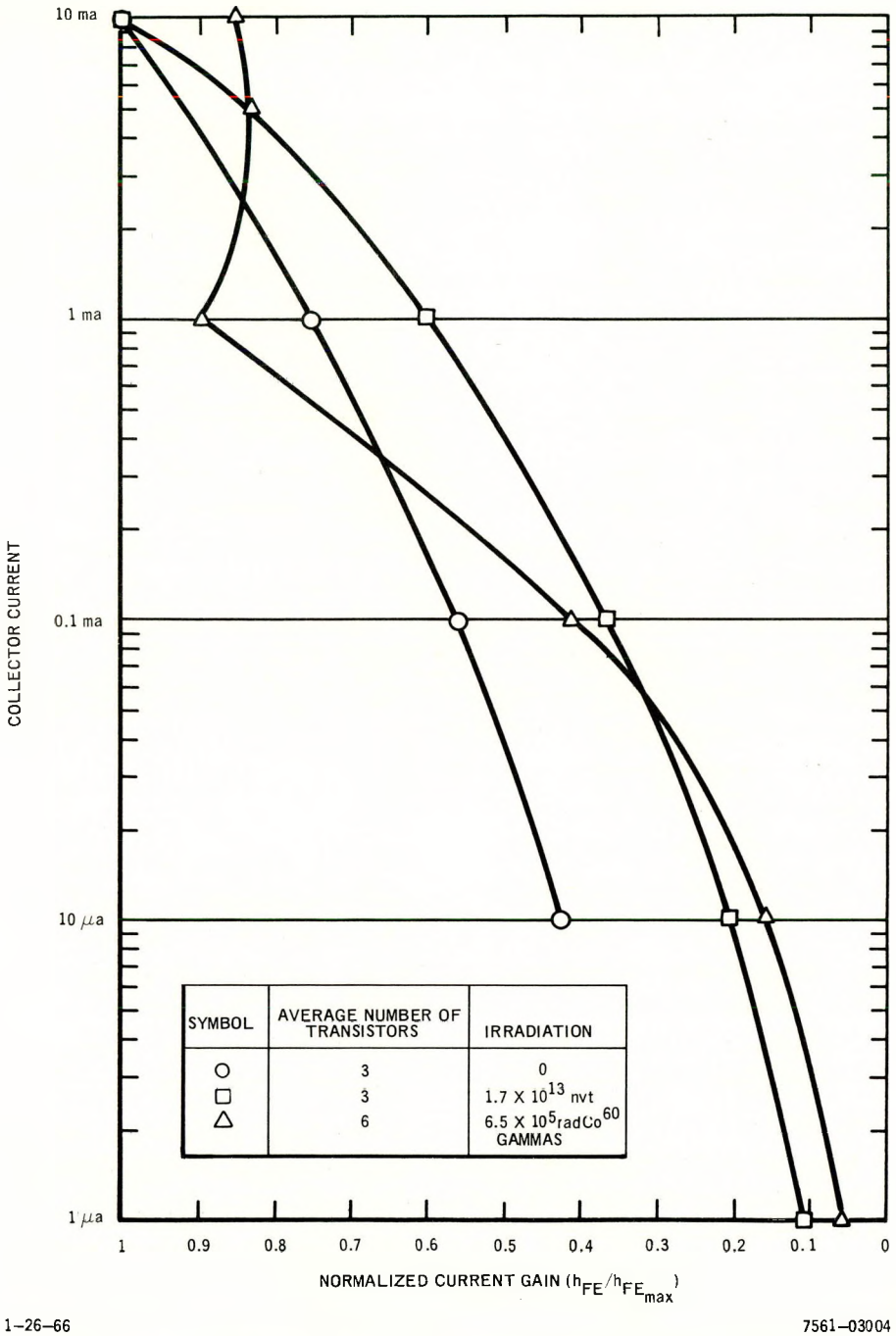

Figure 21. Current-Gain Collector-Current Characteristics

APPENDIX
DETECTOR DATA ANALYSIS TECHNIQUES

The need for a method of evaluating the detector data became apparent as testing was performed at the calculated neutron-gamma ratios of the SNAP 10A instrument compartment environments (2×10^6 to 3×10^7 n/rad). The gamma contribution to the transistor degradation becomes significant at some point between the test conducted at 1.5×10^8 n/rad and the test conducted at 8×10^6 n/rad and necessitates the utilization of a technique to separate the gamma damage from the neutron damage. The gamma susceptibility of the transistors is not characteristic or predictable; therefore, conventional means are not possible. The technique employed herein ignores the effects of the neutron hardening which occurs in traversing several inches of water[10] such as was the case during the in-pool test program at STIR. This may be an assumption with serious shortcomings, since the energy threshold and energy dependence of the 2N697 has not been established experimentally. The technique discussed herein was employed to interpret the FS-4 data with the realization of the limitations of the analysis.

The basis for the analysis is predicated on the assumption that at a neutron-gamma ratio of 1×10^9 n/rad the gamma radiation contribution to the transistor degradation is zero. This appears to be a valid assumption according to the test results at 1.5×10^8 n/rad where the gamma contribution was found to be insignificant. The gamma contribution during the irradiation of eight transistors at STIR at 8×10^6 was determined by expanding the response curve between 12- to 18-mv detector output. The response curves in this range appear to be exhibiting a more uniform degradation rate although there is considerable scatter in the data resulting from the initial difference in the semiconductor susceptibility to gammas. The increased degradation observed during this irradiation was then compared to the reference calibration performed at 1.5×10^8 n/rad by normalizing the data of the eight transistors at 2×10^{12} nvt to 13 mv (Figure 22). The average calibration curve obtained at 1.5×10^8 n/rad was graphed from 12 to 18 mv as was the normalized data for seven transistors irradiated at 8×10^6 n/rad. The arithmetic mean value response of the normalized data for the seven transistors was calculated and this curve plotted to permit comparison with the reference response (Figure 23). The mean value of the normalized data represents an increase in degradation of 37% which corresponds to the best single determination of the gamma contribution for the inconsistent slope of the curve.

The uncertainty in the increased degradation attributable to the gamma radiation was determined from the scatter in the irradiation data (Figure 17) in the region under analysis to be ±25% of the mean normalized value. The uncertainty assigned to the STIR calibration average curve was determined likewise from the composite graph of the six detectors (Figure 12) to be ±15%. The values of uncertainty represent the worst case approximations to determine the upper and lower limits of flux rates.

The basis for gamma corrections has now been established which will permit the gamma contribution to be determined at neutron-gamma ratios between the test conditions of 8×10^6 and 1.5×10^8 n/rad. The gamma contribution at 1.5×10^8 n/rad is approximated initially by direct proportionality of the n/rad ratios at the two test conditions, as follows:

$$\frac{8 \times 10^6 \text{ n/rad}}{1.5 \times 10^8 \text{ n/rad}} = 0.053$$

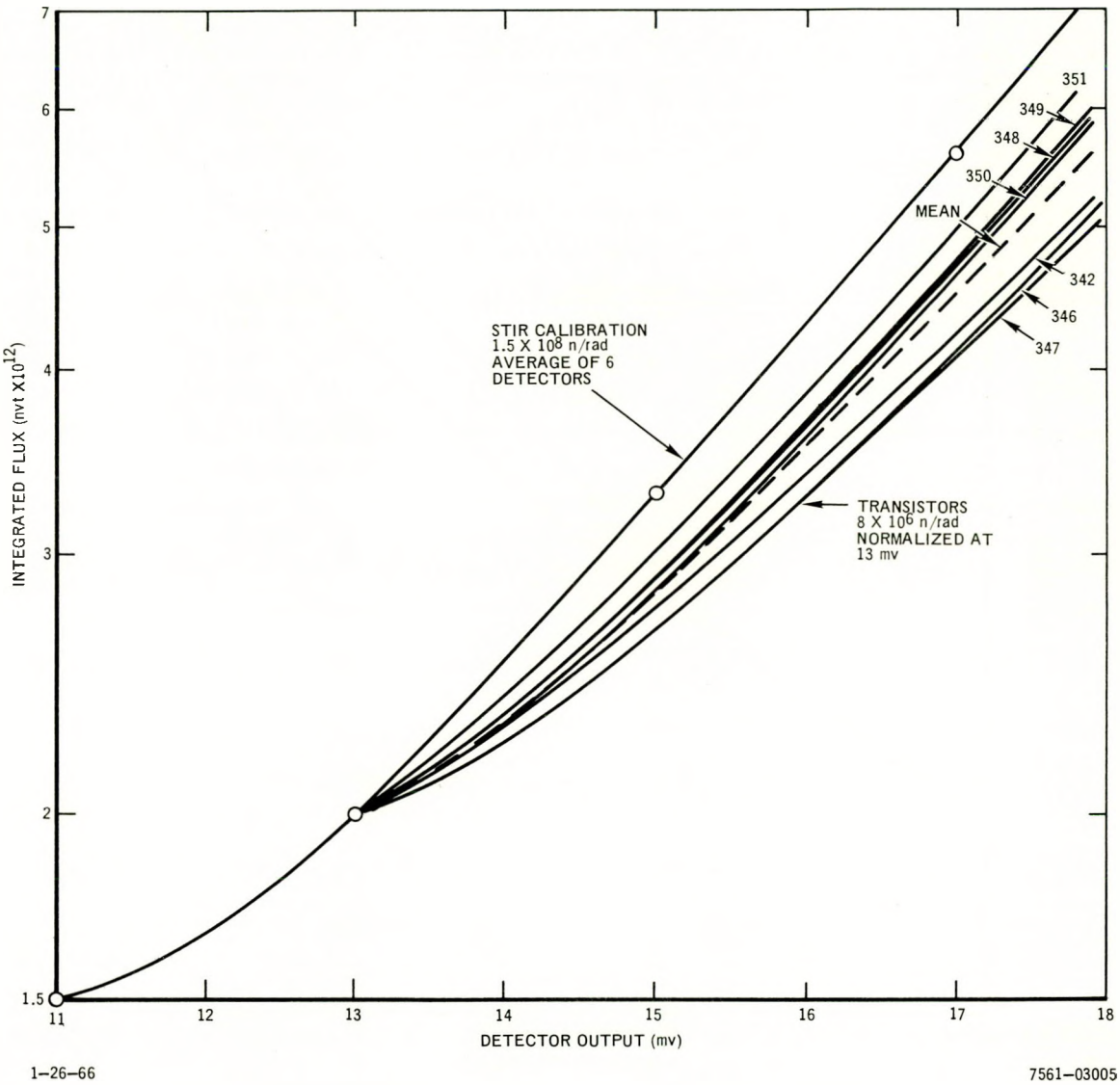

Figure 22. STIR In-Pool Data Normalized to STIR Calibration Data

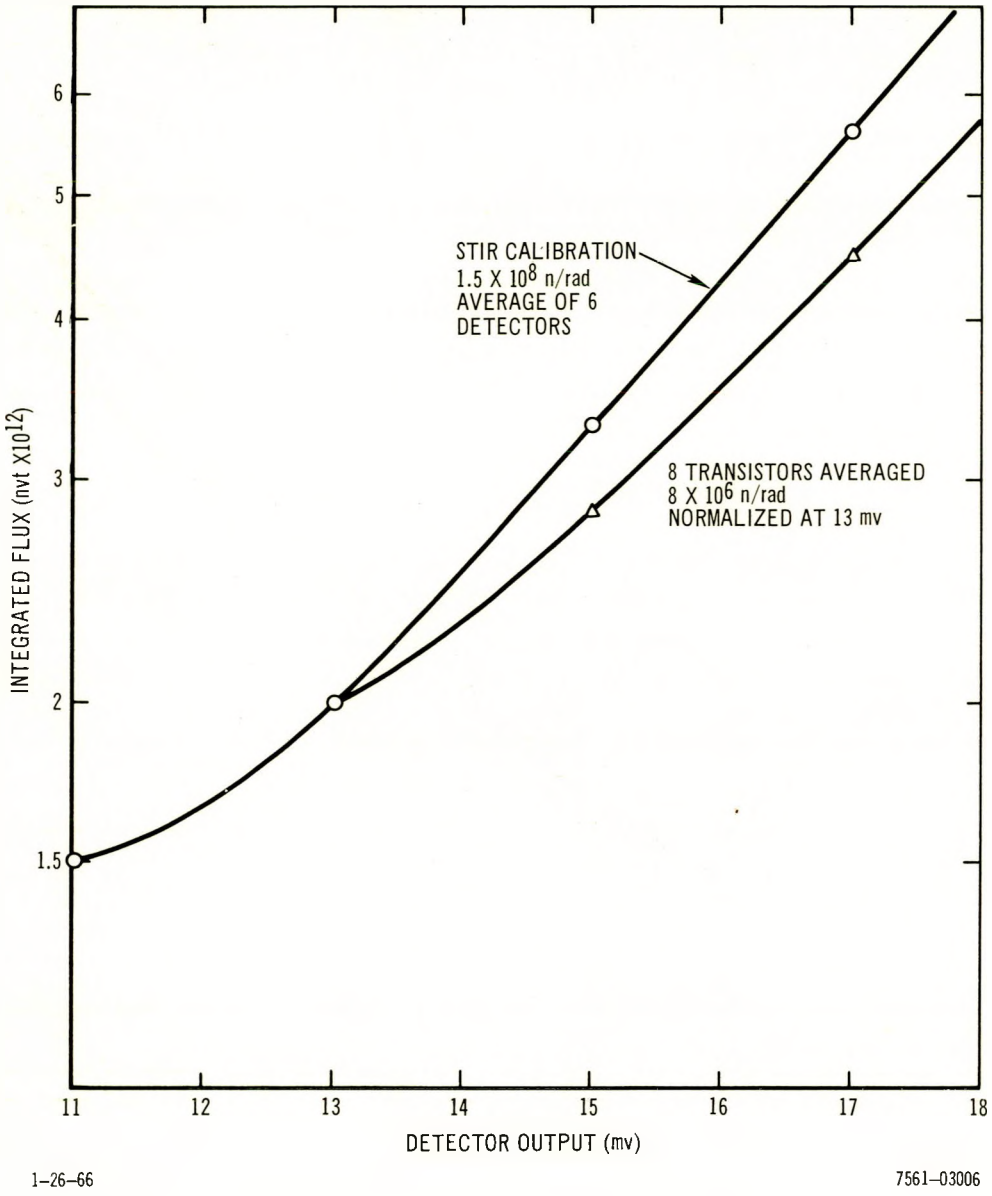

Figure 23. Average Normalized Data

The gamma contribution at 1.5×10^8 = (0.37) x 0.053 - 0.02. This 2% gamma contribution approximation which existed at the reference data condition may now be added to the 37% determination at 8×10^6 n/rad resulting in a total of ~40% degradation increase. A relationship of the corrected degradation of the transistor to the fast neutron flux is expressed in the following formula:

$$\text{corrected nvt (T)} = I - BI$$

where

I = indicated nvt based on the calibration curve at STIR at 1.5×10^8 n/rad,

B = % gamma damage contribution on calibration at various n/rad.

The B value is determined by rationalizing that if the n/rad is increased by a factor of two, then the gamma factor will be reduced by one-half. That is to say, if the gamma damage (b) is 40 parts of the total at 8×10^6 then at 1.6×10^7 n/rad, the gamma factor will be only 20 parts.

b at 8×10^6 n/rad = 40; this leaves 60 attributable to neutron damage and B = 40%, then b at 1.6×10^7 = 20.

Assuming the neutron damage is still 60 parts;

$$B = \frac{b}{60 + b} = \frac{20}{60 + 20} = 25\% \quad ,$$

and

$$T = I - 0.25I \text{ at } 1.6 \times 10^7.$$

This technique was applied for determining the B at neutron-gamma ratios (n/rad) from 1×10^9 to 1×10^6. However, it should be pointed out that below 8×10^6 n/rad this method is extremely questionable. This is due to the fact that between the two test conditions (8×10^6 and 1.5×10^6 n/rad) the response data become meaningless, and the predominant gamma damage results in completely unpredictable transistor characteristics.

The data analysis technique is then used on the FS-4 system where the data indicate a gamma flux of approximately 650 rad/hr. This information may then be multiplied by the neutron-gamma ratio to determine the values of indicated neutron flux at the arbitrary neutron-gamma ratios:

$$\begin{aligned} I &= (\text{n/rad})\,(\text{rad/sec}) \\ &= 8 \times 10^6 (650/3600) \\ &= 1.23 \times 10^6 \text{ n/cm}^2\text{-sec} \quad . \end{aligned}$$

Then

$$T = I - BI$$

$$T = 1.23 \times 10^6 - (40)\,(1.23 \times 10^6) = 0.74 \times 10^6.$$

This calculation is performed for several neutron-gamma ratios and a correction curve generated which permits the corrected flux to be determined at the values of indicated flux defined by the calibration curve at 1.5×10^8 n/rad for similar detectors. This correction curve is shown on Figure 24.

The uncertainty band of this correction curve is determined by calculations based on the previous values of uncertainty in the reference calibration curve at 1.5×10^8 n/rad and the normalized data at 8×10^6 n/rad which was ±15% and ±25% respectively.

$$T = (I \pm 0.15I) - (B \pm 0.25B)\,(I \pm 0.15I)$$

Simplifying for extreme cases:

$$T_{min} = (I - 0.15I) - (1.44BI),$$

$$T_{max} = (I + 0.15I) - (0.64BI),$$

$$T_{min} = (1.23 \times 10^6 - 0.184 \times 10^6) - (1.44 \times 0.492),$$

$$T_{min} = 0.34 \times 10^6 \text{ n/cm}^2\text{-sec},$$

$$T_{max} = 1.10 \times 10^6 \text{ n/cm}^2\text{-sec}.$$

This final step has provided a correction curve for FS-4 indicated neutron fluxes to be made with the appreciation of the uncertainty of the corrected values.

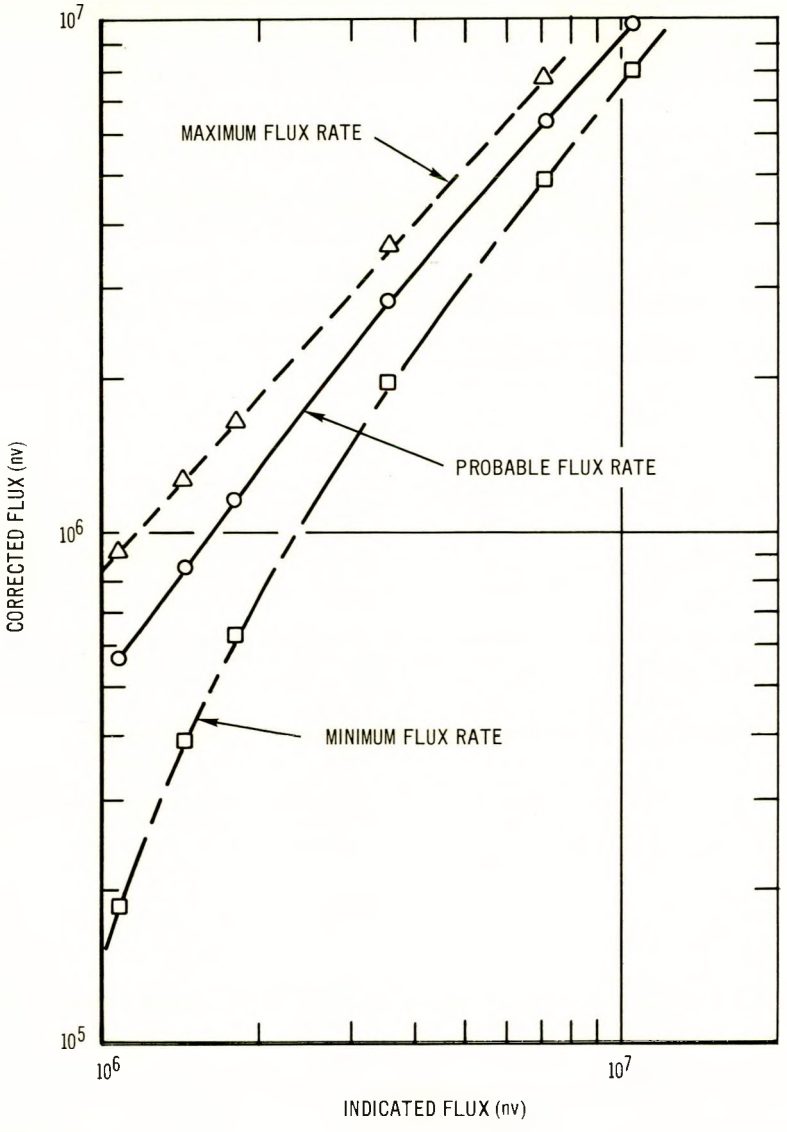

Figure 24. Gamma Correction Curve

REFERENCES

1. J. A. Belcher, W. A. Flynn, and R. J. Thomson, "SNAP 10A Radiation Shield Analysis," NAA-SR-9647 (October 15,1964)

2. R. R. Blair, "Surface Effects of Radiation on Transistors," IEEE Transactions on Nuclear Science, Vol. NS-10, No. 5 (November 1963)

3. Peder J. Estrup, "Surface Effects of Gaseous Ions and Electrons on Semiconductor Devices," IEEE Transactions on Nuclear Science, Vol. NS-12, No. 1 (February 1965)

4. The Bell System Technical Journal, Vol. 42 (July 1963)

5. F. Larin and F. Pollenz, "Summary of Behavior of Selected Transistors in Radiation Environments," Bendix Corp. Research Laboratories Div., Report No. 2696

6. F. Larin and D. J. Niehaus, "Damage by Radiation," Bendix Corp. Research Laboratories, Nucleonics (September 1964)

7. G. E. Transistor Manual, Sixth Edition, Page 234

8. R. R. Brown, "Proton and Electron Permanent Damage in Silicon Semiconductor Devices," ANS-ASTM Conference on Radiation Effects in Electronics, Syracuse, N.Y. (October 5-7, 1964)

9. M. N. Robinson, "Comparison of Neutron and Gamma Radiation Damage in Semiconductors," NAA-SR-10856 (December 28, 1964)

10. "Annual Progress Report for Period Ending August 1, 1963," ORNL-3499, Vol. 1, Neutron Physics Division, ORNL

11. M. N. Robinson, "Radiation Damage in Silicon, Neutron Spectrum Considerations," NAA-SR-10612 (October 27, 1964)

12. BNL 325, Neutron Cross Sections

13. S. G. Wogulis and K. L. Rooney, "Experimental Studies of Neutron Attenuation in Material Lithium Hydride Shields," NAA-SR-9364 (February 12, 1964)